

1 **Neural speech tracking benefit of lip movements predicts**
2 **behavioral deterioration when the speaker's mouth is**
3 **occluded**

4 Patrick Reisinger^{1*}, Marlies Gillis², Nina Suess¹, Jonas Vanthornhout², Chandra Leon Haider¹,
5 Thomas Hartmann¹, Anne Hauswald¹, Konrad Schwarz³, Tom Francart^{2†}, Nathan Weisz^{1,4†}

6 ¹Paris-Lodron-University of Salzburg, Department of Psychology, Centre for Cognitive
7 Neuroscience, Salzburg, Austria

8 ²Experimental Oto-Rhino-Laryngology, Department of Neurosciences, Leuven Brain Institute,
9 KU Leuven, Leuven, Belgium

10 ³MED-EL GmbH, Innsbruck, Austria

11 ⁴Neuroscience Institute, Christian Doppler University Hospital, Paracelsus Medical University
12 Salzburg, Salzburg, Austria

13 *Corresponding author: patrick.reisinger@plus.ac.at

14 †Shared last authorship

15 **Abstract**

16 Observing lip movements of a speaker is known to facilitate speech understanding, especially in
17 challenging listening situations. Converging evidence from neuroscientific studies shows
18 enhanced processing of audiovisual stimuli. However, the interindividual variability of this visual
19 benefit and its consequences on behavior are unknown. Here, we analyzed source-localized
20 magnetoencephalographic (MEG) responses from normal-hearing participants listening to
21 audiovisual speech with or without an additional distractor speaker. Using temporal response
22 functions (TRFs), we show that neural responses to lip movements are, in general, enhanced
23 when speech is challenging. After conducting a crucial control for speech acoustics, we show that
24 lip movements effectively contribute to higher neural speech tracking, particularly when a
25 distractor speaker is present. However, the extent of this visual benefit varied greatly among
26 participants. Probing the behavioral relevance, we show that individuals who benefit more from
27 lip movement information in terms of neural speech tracking, show a stronger drop in performance
28 and an increase in perceived difficulty when the mouth is occluded by a surgical face mask. By
29 contrast, no effect was found when the mouth was not occluded. We provide novel insights on
30 how the benefit of lip movements in terms of neural speech tracking varies among individuals.
31 Furthermore, we reveal its behavioral relevance by demonstrating negative consequences for
32 behavior when visual speech is absent. Our results also offer potential implications for future
33 objective assessments of audiovisual speech perception.

34 Introduction

35 Face masks are an important tool in preventing the spread of contagious diseases such as
36 COVID-19 (e.g. Chu et al., 2020; Suñer et al., 2022). However, as many have subjectively
37 experienced first hand, the use of face masks also impairs speech perception, and not only by
38 attenuating sound. More importantly, they occlude facial expressions, such as lip movements
39 (e.g. Brown et al., 2021; Rahne et al., 2021), that provide visual information for a relevant speech
40 stream. This is particularly critical when speech is challenging, such as in the classic cocktail party
41 situation, where multiple conversations are happening simultaneously (Cherry, 1953). In such
42 situations, the brain separates auditory information of interest from competing input (McDermott,
43 2009). Ideally, visual information is available to support this process, with numerous studies
44 demonstrating that visual speech features enhance the understanding of degraded auditory input
45 (e.g. Grant & Seitz, 2000; Remez, 2012; Ross et al., 2007; Sumbly & Pollack, 1954). This concept
46 is known as inverse effectiveness (Meredith & Stein, 1983; van de Rijt et al., 2019). Among visual
47 speech features, lip movements are the most important, playing a crucial role in the perception of
48 challenging speech (Erber, 1975; Peelle & Sommers, 2015). This is especially intriguing given
49 the substantial interindividual differences in lip-reading performance among normal, as well as
50 hearing-impaired, populations (Suess, Hauswald, Zehentner, et al., 2022; Summerfield et al.,
51 1992). Despite our imperfect lip-reading abilities, the human brain effectively uses lip movements
52 to facilitate the perception of challenging speech, with the neural mechanisms and regions
53 involved still under debate (Ross et al., 2022; Zhang & Du, 2022).

54 Previous studies have shown beneficial effects of visual speech on the representation of speech
55 in the brain. An MEG study by Park et al. (2016) showed enhanced entrainment between lip
56 movements and speech-related brain areas when congruent audiovisual speech was presented.
57 Other studies have shown that the incorporation of visual speech enhances the ability of the brain
58 to track acoustic speech (Crosse et al., 2015; Crosse, Liberto, et al., 2016; Golumbic et al., 2013).
59 Interestingly, when silent lip movements are presented, the brain also tracks the unheard acoustic
60 speech envelope (e.g. Hauswald et al., 2018) or spectral fine details (Suess, Hauswald,
61 Reisinger, et al., 2022). Despite these findings, two questions remain unanswered: First, it is
62 unknown how individuals vary in their benefit of lip movements at the neural level. Given the
63 aforementioned interindividual differences in lip-reading performance, a high degree of variability
64 could also be expected here. Importantly, lip movements are correlated with acoustic speech
65 features (Chandrasekaran et al., 2009), so it is essential to control for acoustic-related brain

66 activity. Second, it is unknown if the individual benefit of lip movements is of behavioral relevance,
67 as, for example, when the lips are occluded with a face mask, as has been common during the
68 COVID-19 pandemic. Given the negative impact of face masks on behavioral measures (e.g.
69 Rahne et al., 2021; Toscano & Toscano, 2021; Truong et al., 2021), a relationship is plausible:
70 Individuals who benefit more should, in principle, also show poorer behavioral outcomes when no
71 lip movements are available, as they are deprived of critical visual information.

72 A suitable method to obtain the individual benefit of lip movements is neural tracking (Obleser &
73 Kayser, 2019). Besides frequency-based coherence and mutual information, temporal response
74 functions (TRFs) have gained widespread popularity (Brodbeck & Simon, 2020; Crosse et al.,
75 2021). TRFs typically aim to predict the M/EEG-recorded neural response to one or more stimulus
76 features, and the prediction is correlated with the original signal to quantify neural tracking. This
77 approach has so far extended our understanding of speech processing from acoustic features
78 (Lalor et al., 2009) to higher-level linguistic features (Brodbeck, Hong, et al., 2018; Broderick et
79 al., 2018; Gillis et al., 2021). Crucially, neural tracking can be used to disentangle the
80 aforementioned intercorrelation of audiovisual speech by controlling for acoustic speech features
81 (Gillis et al., 2022). This could reveal the “pure” individual benefit of lip movements to neural
82 speech tracking in audiovisual settings, which has not yet been shown.

83 Neural speech tracking has been proposed as an objective measure for speech intelligibility
84 (Schmitt et al., 2022; Vanthornhout et al., 2018) along with a whole range of auditory and linguistic
85 processes (Gillis et al., 2022). Previously, acoustic neural speech tracking has been related to
86 behavioral measures such as speech intelligibility (Chen et al., 2023; Ding & Simon, 2013).
87 Studies that involve visual speech features have established a relationship between the neural
88 tracking of visual speech cues, so-called visemes, and lip-reading performance (Nidiffer et al.,
89 2021) or lip movements and speech comprehension (Park et al., 2016). In sum, these findings
90 strongly suggest a meaningful relationship between neural speech tracking and behavioral
91 measures. Regarding the aspect of interindividual differences, Schubert et al. (2023) showed that
92 the MEG-derived tendency of individuals to predict upcoming tones facilitates neural speech
93 tracking, and this relationship generalizes to various audio-only listening situations. Here, we aim
94 to combine both aspects by evaluating the relationship between interindividual differences and
95 behavioral measures. In particular, we probe the behavioral relevance of the individual benefit of
96 lip movements, especially when critical visual information is not available. Addressing this could
97 further strengthen the case for the behavioral relevance of neural speech tracking as an objective
98 measure of speech processing.

99 Here, we used MEG and an audiovisual speech paradigm with one or two speakers to investigate
100 the benefit of lip movements and its behavioral relevance. Utilizing a state-of-the-art neural
101 tracking framework with source-localized TRFs (see Figure 1), we show that lip movements are
102 processed more strongly when speech is challenging. Additionally, we show that the neural
103 tracking of lip movements is enhanced in multi speaker settings. When controlled for acoustic
104 speech features, the obtained benefit of lip movements is, in general, more enhanced in the multi
105 speaker condition, with substantial interindividual variability. Using Bayesian modeling, we show
106 that acoustic speech tracking is related to behavioral measures. Crucially, we demonstrate that
107 individuals who benefit more from lip movements show a stronger drop in performance and report
108 a higher subjective difficulty when the mouth is occluded by a surgical face mask. In terms of
109 neural tracking, our results suggest that individuals benefit from lip movements in a highly variable
110 manner. We also establish a novel link between the neural benefit of visual speech and behavior
111 when no visual speech information is available.

112 **Material and Methods**

113 *Participants*

114 The data was collected as part of a recent study (Haider et al., 2022), in which 30 native speakers
115 of German participated. One participant was excluded because signal source separation could
116 not be applied to the MEG dataset. This led to a final sample size of 29 participants (12 females,
117 $M_{\text{age}} = 26.79$, $SD_{\text{age}} = 4.87$ years). All participants reported normal vision and hearing (thresholds
118 did not exceed 25 dB HL at any frequency from 125 to 8000 Hz), the latter verified by a standard
119 clinical audiometer (AS608 Basic; Interacoustics A/S, Middelfart, Denmark). Additional exclusion
120 criteria included non-removable magnetic objects and any psychiatric or neurologic history. All
121 participants signed an informed consent and were reimbursed at a rate of 10 € per hour. The
122 experimental protocol was approved by the ethics committee of the Paris-Lodron-University of
123 Salzburg and was conducted in accordance with the Declaration of Helsinki.

124 *Stimuli and experimental design*

125 The experimental procedure was implemented in MATLAB 9.10 (The MathWorks Inc., Natick,
126 Massachusetts, USA) using custom scripts. Presentation of stimuli and response collection was
127 achieved with the Objective Psychophysics Toolbox (o_ptb; Hartmann & Weisz, 2020), which
128 adds a class-based abstraction layer onto the Psychophysics Toolbox version 3.0.16 (Brainard,

129 1997; Kleiner et al., 2007; Pelli, 1997). Stimuli and triggers were generated and emitted via the
130 VPixx system (DATAPixx2 display driver, PROPixx DLP LED projector, RESPONSEPixx
131 response box by VPixx Technologies Inc., Saint-Bruno, Canada). Videos were back-projected
132 onto a translucent screen with a screen diagonal of 74 cm (~110 cm in front of the participants),
133 with a refresh rate of 120 Hz and a resolution of 1920×1080 pixels. Timings were measured with
134 the Black Box ToolKit v2 (The Black Box ToolKit Ltd., Sheffield, UK) to ensure accurate stimulus
135 presentation and triggering.

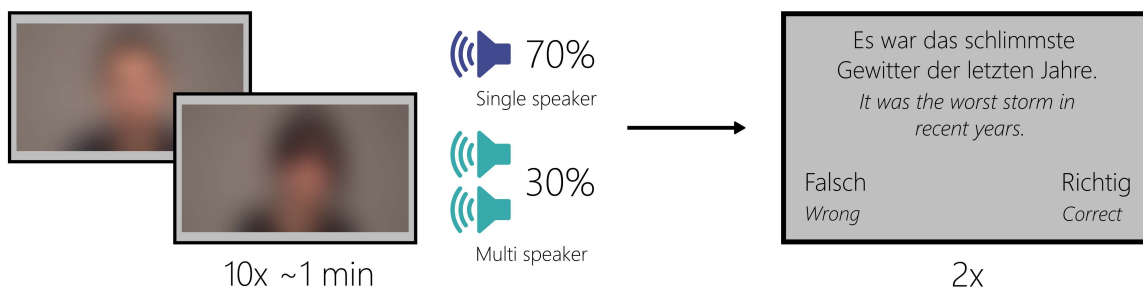
136 The audiovisual stimuli were excerpts from four German stories, two of each read out loud by a
137 female or male speaker (female: "Die Schokoladenvilla - Zeit des Schicksals. Die Vorgeschichte
138 zu Band 3" by Maria Nikolai, "Die Federn des Windes" by Manuel Timm; male: "Das Gestüt am
139 See. Charlottes großer Traum" by Paula Mattis and "Gegen den Willen der Väter" by Klaus
140 Tiberius Schmidt). A Sony NEX-FS100 (Sony Group Corporation, Tokyo, Japan) camera with a
141 sampling rate of 25 Hz and a RØDE NTG2 microphone (RØDE Microphones Pty. Ltd., Sydney,
142 Australia) with a sampling rate of 48 kHz were used to record the stimuli. Each of the four stories
143 was recorded twice, once with and once without a surgical face mask (type IIR three-layer
144 disposable medical mask). These eight videos were cut into 10 segments of about one minute
145 each ($M = 64.29$ s, $SD = 4.87$ s), resulting in 80 videos. In order to rule out sex-specific effects,
146 40 videos (20 with a female speaker and 20 with a male speaker) were presented to each
147 participant. The speakers' syllable rates were analyzed using Praat (Boersma, 2001; de Jong &
148 Wempe, 2009) and varied between 3.7 Hz and 4.6 Hz ($M = 4.1$ Hz). The audio-only distractor
149 speech consisted of pre-recorded audiobooks (see Schubert et al., 2023), read by either a female
150 or a male speaker.

151 Before the experiment, a standard clinical audiometry was performed (for details, see
152 *Participants*). The MEG measurement started with a 5-minute resting-state recording (not
153 analyzed in this manuscript). Next, the participant's individual hearing threshold was determined
154 in order to adjust the stimulation volume. If the participant reported that the stimulation was not
155 loud enough or comfortable, the volume was manually adjusted to the participant's requirements.

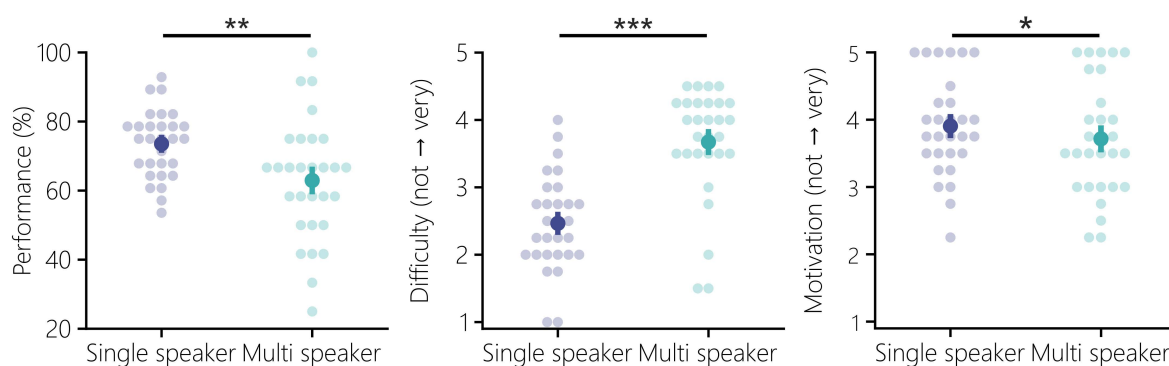
156 The actual experiment consisted of four stimulation blocks, one for each of the four stories, with
157 two featuring each sex. Each story was presented as a block of 10 ~one-minute trials in
158 chronological order to preserve the story content (Figure 1A). In every block, a same-sex audio-
159 only distractor speaker was added to three randomly selected trials, with a 5-second delay and
160 volume equal to the target speaker. The resulting ratio of 30% multi speaker trials and 70% single

161 speaker trials per block was chosen because of a different data analysis method in Haider et al.
162 (2022). The distractor speech started with a delay of 5 seconds to give participants time to attend
163 the target speaker. In two randomly selected blocks, the target speaker wore a face mask (only
164 the corresponding behavioral data was used here, see *Statistical analysis and Bayesian*
165 *modeling*). Two unstandardized correct or wrong statements about semantic content were
166 presented after each trial to assess comprehension performance and to maintain attention (Figure
167 1A). On four occasions in each block, participants also rated subjective difficulty and motivation
168 on a five-point Likert scale (not depicted in Figure 1A). The participants responded by pressing
169 buttons. The total duration of the experiment was ~2 h, including preparation.

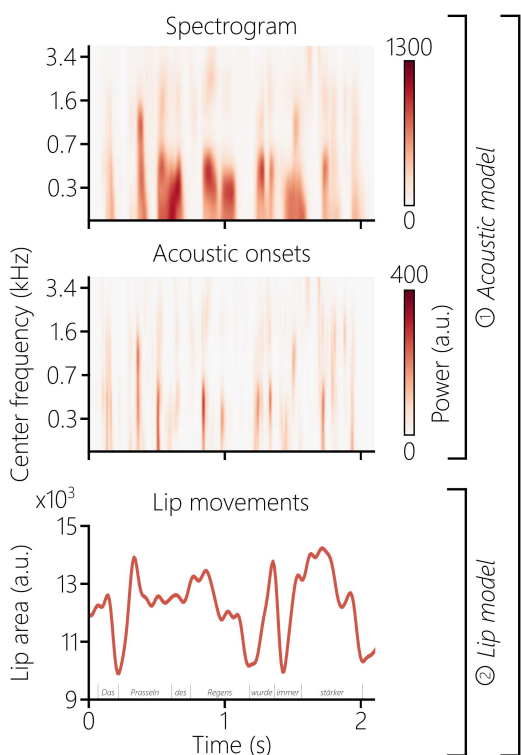
A) Audiovisual speech **Comprehension statements**



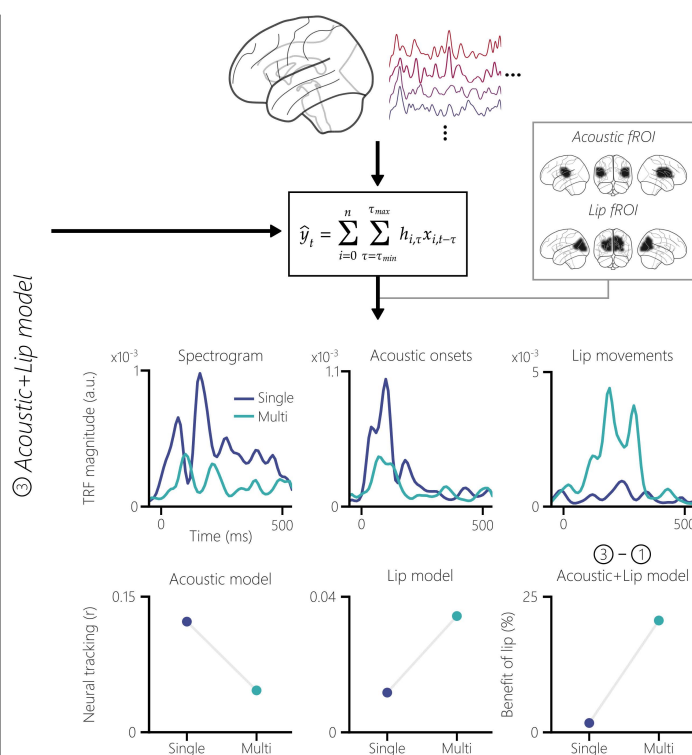
B) Performance **Difficulty** **Motivation**



C) Stimulus features



Forward models



170 **Figure 1.** *Experimental design, behavioral results and analysis framework.* (A) Each block consisted of 10
171 ~1-min trials of continuous audiovisual speech by either a female or male speaker (single speaker
172 condition). In 30% of these 10 trials, a same-sex audio-only distractor speaker was added (multi speaker
173 condition). After every block, two comprehension statements had to be rated as correct or wrong. (B)
174 Performance on the comprehension statements in the multi speaker condition was lower than in the single
175 speaker condition ($p = .003$, $r_C = 0.64$). Subjective difficulty ratings, reported on a five-point Likert scale,
176 were higher in the multi speaker condition ($p = 9.00e^{-06}$, $r_C = -0.95$). The reported motivation was lower in
177 the multi speaker condition ($p = .024$, $r_C = 0.62$). The middle dots represent the mean, and the bars, the
178 standard error of the mean. (C) Three stimulus features (spectrogram, acoustic onsets and lip movements)
179 extracted from the audiovisual stimuli are shown for an example sentence. Higher values in the lip area unit
180 represent a wider opening of the mouth and vice versa. Three forward models were calculated: (1) one
181 using only acoustic features, (2) one using only lip movements, and (3) one combining all features. Together
182 with the corresponding source-localized MEG data, the boosting algorithm was used to calculate the
183 models. Exemplary minimum-norm source estimates are shown for a representative participant. The
184 resulting TRFs (a.u.) and neural tracking (expressed as Pearson's r) were analyzed in functional regions of
185 interest (fROIs), obtained either via the acoustic or lip model of the multi speaker condition. The TRFs and
186 prediction accuracies shown are from a representative participant reflecting the group-level results. To
187 obtain the benefit of lip movements, acoustic features were controlled by subtracting the prediction
188 accuracies in an acoustic+lip fROI of the acoustic model from the combined model. The benefit of lip
189 movements was expressed as a percentage change. * $p < .05$, ** $p < .01$, *** $p < .001$; *Speakers have been*
190 *blurred due to a bioRxiv policy on the inclusion of faces.*

191 *MEG data acquisition and preprocessing*

192 Before entering the magnetically shielded room, five head position indicator (HPI) coils were
193 applied on the scalp. Electrodes for electrooculography (EOG; vertical and horizontal eye
194 movements) and electrocardiography (ECG) were also applied (recorded data not used here).
195 Fiducial landmarks (nasion and left/right pre-auricular points), the HPI locations and ~300 head
196 shape points were sampled with a Polhemus FASTRAK digitizer (Polhemus, Colchester,
197 Vermont, USA).

198 Magnetic brain activity was recorded with a Neuromag Triux whole-head MEG system (MEGIN
199 Oy, Espoo, Finland) using a sampling rate of 1000 Hz (hardware filters: 0.1-330 Hz). The signals
200 were acquired from 102 magnetometers and 204 orthogonally placed planar gradiometers at 102
201 different positions. The system is placed in a standard passive magnetically shielded room (AK3b;
202 Vacuumschmelze GmbH & Co. KG, Hanau, Germany).

203 A signal space separation (SSS; Taulu & Kajola, 2005; Taulu & Simola, 2006) algorithm
204 implemented in MaxFilter version 2.2.15 provided by the MEG manufacturer was used. The
205 algorithm removes external noise from the MEG signal (mainly 16.6 Hz, and 50 Hz, plus
206 harmonics) and realigns the data to a common standard head position (to [0 0 40] mm, *-trans*
207 *default* MaxFilter parameter) across different blocks, based on the measured head position at the
208 beginning of each block.

209 Preprocessing of the raw data was done in MATLAB 9.8 using the FieldTrip toolbox (revision
210 f7adf3ab0; Oostenveld et al., 2011). A low-pass filter of 10 Hz (hamming-windowed sinc FIR filter,
211 onepass-zero phase, order: 1320, transition width: 2.5 Hz) was applied, and the data was
212 downsampled to 100 Hz. Afterwards, a high-pass filter of 1 Hz (hamming-windowed sinc FIR filter,
213 onepass-zero phase, order: 166, transition width: 2.0 Hz) was applied.

214 Independent component analysis (ICA) was used to remove eye and cardiac artifacts (data was
215 filtered between 1-100 Hz, sampling rate: 1000 Hz) via the infomax algorithm (“runica”
216 implementation in EEGLAB; Bell & Sejnowski, 1995; Delorme & Makeig, 2004) applied to a
217 random block of the main experiment. Prior to the ICA computation, we performed a principal
218 component analysis (PCA) with 50 components in order to ease the convergence of the ICA
219 algorithm. After visual identification of artifact-related components, an average of 2.38
220 components per participant were removed (SD = 0.68).

221 The cleaned data was epoched into trials that matched the length of the audiovisual stimuli. To
222 account for an auditory stimulus delay introduced by the tubes of the sound system, the data were
223 shifted by 16.5 ms. In the multi speaker condition, the first 5 seconds of data were removed to
224 match the onset of the distractor speech. The last eight trials were removed to equalize the data
225 length between the single speaker and multi speaker conditions. To prepare the data for the
226 following steps, the trials in each condition were concatenated. This resulted in a data length of
227 ~6 min per condition.

228 *Source localization*

229 Source projection of the data was done with MNE-Python 1.1.0 running on Python 3.9.7 (Gramfort
230 et al., 2013, 2014). A semi-automatic coregistration pipeline was used to coregister the FreeSurfer
231 “fsaverage” template brain (Fischl, 2012) to each participant's head shape. After an initial fit using
232 the three fiducial landmarks, the coregistration was refined with the Iterative Closest Point (ICP)
233 algorithm (Besl & McKay, 1992). Head shape points that were more than 5 mm away from the

234 scalp were automatically omitted. The subsequent final fit was visually inspected to confirm its
235 accuracy. This semi-automatic approach performs comparably to manual coregistration pipelines
236 (Houck & Claus, 2020).

237 A single-layer boundary element model (BEM; Akalin-Acar & Gençer, 2004) was computed to
238 create a BEM solution for the “fsaverage” template brain. Next, a volumetric source space with a
239 grid of 7 mm was defined, containing a total of 5222 sources (Kulasingham et al., 2020). In order
240 to remove non-relevant regions and shorten computation times, subcortical structures along the
241 midline were removed, reducing the source space to 3053 sources (similar to Das et al., 2020).
242 Subsequently, the forward operator (i.e. lead field matrix) was computed using the individual
243 coregistrations, the BEM and the volume source space.

244 Afterwards, the data were projected to the defined sources using the Minimum Norm Estimate
245 method (MNE; Hämäläinen & Ilmoniemi, 1994). MNE is known to be biased towards superficial
246 sources, which can be reduced by applying depth weighting with a coefficient between 0.6 and
247 0.8 (Lin et al., 2006). For creating the MNE inverse operator, depth weighting with a coefficient of
248 0.8 was used (e.g. Brodbeck et al., 2018). The required noise covariance matrix was estimated
249 with an empty-room MEG recording relative to the participant’s measurement date with the same
250 preprocessing settings as the MEG data of the actual experiment (see *MEG data acquisition and*
251 *preprocessing*). The MNE inverse operator was then applied to the concatenated MEG data with
252 ℓ_2 regularization (signal-to-noise ratio (SNR) = 3 dB, $\lambda^2 = \frac{1}{SNR^2}$) and three free-orientation dipoles
253 orthogonally at each source.

254 *Extraction of stimulus features*

255 Since the focus of this study is on audiovisual speech, we extracted acoustic (spectrograms and
256 acoustic onsets) and visual (lip movements) speech features from the stimuli (for examples see
257 Figure 1C). The spectrograms of the auditory stimuli were obtained using the Gammatone
258 Filterbank Toolkit 1.0 (Heeris, 2013), with frequency cutoffs at 20 and 5000 Hz, 256 filter channels
259 and a window time of 0.01 s. This toolkit computes a spectrogram representation on the basis of
260 a set of Gammatone filters which are inspired by the human auditory system (Slaney, 1998). The
261 resulting filter outputs with logarithmic center frequencies were averaged into eight frequency
262 bands (frequencies <100 Hz were omitted; Gillis et al., 2021). Each frequency band was scaled
263 with exponent 0.6 (Biesmans et al., 2017) and downsampled to 100 Hz, which is the same
264 sampling frequency as the preprocessed MEG data.

265 Acoustic onset representations were calculated for each frequency band of the spectrograms
266 using an auditory edge detection model (Fishbach et al., 2001). The resulting spectrograms of
267 the acoustic onsets are valuable predictors of MEG responses to speech stimuli (Brodbeck et al.,
268 2020; Daube et al., 2019). A delay layer with 10 delays from 3 to 5 ms, a saturation scaling factor
269 of 30 and a receptive field based on the derivative of a Gaussian window (SD = 2 ms) were used
270 (Gillis et al., 2021). Each frequency band was downsampled to 100 Hz.

271 The lip movements of every speaker were extracted from the videos with a MATLAB script
272 adapted from Suess et al. (2022; originally by Park et al., 2016). Within the lip contour, the area,
273 and the horizontal and vertical axis were calculated. Only the area was used for the analysis,
274 which leads to results comparable to using the vertical axis (Park et al., 2016). The lip area signal
275 was upsampled from 25 Hz to 100 Hz using FFT-based interpolation.

276 *Forward models*

277 A linear forward modeling approach was used to predict the MEG response to the aforementioned
278 stimulus features (see Figure 1C). These approaches are based on the idea that the brain's
279 response to a stimulus is a continuous function in time (Lalor et al., 2006). The boosting algorithm
280 (David et al., 2007), implemented in eelbrain 0.38 (running on Python 3.9.7; Brodbeck et al.,
281 2022), was used to predict MNE source-localized MEG responses to stimulus features ("MNE-
282 boosting"; Brodbeck, Presacco, et al., 2018). For multiple stimulus features, the linear forward
283 model can be formulated as:

$$284 \quad \hat{y}_t = \sum_{i=0}^n \sum_{\tau=\tau_{min}}^{\tau_{max}} h_{i,\tau} x_{i,t-\tau}$$

285 For every n stimulus feature, the algorithm finds an optimal filter kernel h , which is also known as
286 a temporal response function (TRF). When n stimulus features is > 1 , h is referred to as
287 multivariate TRF (mTRF). The term τ denotes the delays between the predicted brain response
288 \hat{y}_t and stimulus feature x (for further details see Brodbeck et al., 2022). TRFs reflect responses
289 to continuous data instead of averaged responses to discrete events (Crosse et al., 2021). For
290 the estimation of the TRFs, the stimulus features and MEG data were normalized (z-scored), and
291 an integration window from -100 to 600 ms with a kernel basis of 50 ms Hamming windows was
292 defined. To prevent overfitting, early stopping based on the ℓ_2 norm was used. By using four-fold
293 nested crossvalidation (two training folds, one validation fold, and one test fold), each partition

294 served as a test set once (Brodbeck et al., 2022). TRFs were estimated for each of the three free-
295 orientation dipoles independently at all 3053 sources (see *Source localization*). The spectrogram
296 and acoustic onset mTRFs were averaged over the frequency dimension. To account for
297 interindividual anatomical differences, TRFs were spatially smoothed with a Gaussian kernel (SD
298 = 5 mm; Kulasingham et al., 2020). The vector norm of the smoothed TRFs was taken, resulting
299 in one TRF per source.

300 To obtain a measure of neural tracking, the predicted brain response \hat{y}_t is correlated with the
301 original response to calculate the prediction accuracy and computed as the average dot product
302 over time (expressed as Pearson correlation coefficient r). This correlation can be interpreted as
303 follows: The higher the prediction accuracy, the higher the neural tracking (Gillis et al., 2022).

304 In order to investigate the neural processing of the audiovisual speech features, we calculated
305 three different forward models per condition and participant (see Figure 1C for the analysis
306 framework). The acoustic model consisted of the two acoustic stimulus features (spectrogram
307 and acoustic onsets) and – also applicable to all other models – the corresponding MNE source-
308 localized MEG data. The lip model contained only the lip movements as a stimulus feature.
309 Additionally, a combined acoustic+lip model was calculated to control for acoustic features in a
310 subsequent analysis.

311 We defined functional regions of interest (fROIs; Nieto-Castanon et al., 2003) by creating labels
312 based on the 90th percentile of the whole-brain prediction accuracies in the multi speaker
313 condition (similar to Suess, Hauswald, Reisinger, et al., 2022). The multi speaker condition was
314 chosen for extracting the fROIs because it potentially incorporates all included stimulus features,
315 due to its higher demand (Golumbic et al., 2013). This was done separately for the acoustic and
316 lip models to map their unique neural sources (see Figure 1C). According to the “aparc”
317 FreeSurfer parcellation (Desikan et al., 2006), the acoustic fROI mainly involved sources in the
318 temporal, lateral parietal and posterior frontal lobes. The superior parietal and lateral occipital
319 lobes made up the majority of the lip fROI. To obtain an audiovisual fROI for the acoustic+lip
320 model, we combined the labels of the acoustic and lip fROIs.

321 For every model, the TRFs in their respective fROI were averaged and, exclusively for Figure 2A,
322 smoothed over time with a 50 ms Hamming window. Grand-average TRF magnitude peaks were
323 detected with scipy version 1.8.0 (running on Python 3.9.7; Virtanen et al., 2020) and visualized
324 as a difference between the multi and single speaker conditions. To suppress regression artifacts
325 that typically occur (Crosse, Di Liberto, et al., 2016), TRFs were visualized between -50 and 550

326 ms. Prediction accuracies in the fROIs were Fisher z-transformed, then averaged, and then the
327 z-values were back-transformed to Pearson correlation coefficients (Corey et al., 1998). For the
328 lower panels of each model in Figure 2B, the prediction accuracies of the acoustic and lip models
329 were averaged in their respective fROIs. Figures were created with the built-in plotting functions
330 of eelbrain and seaborn version 0.12.0 (running on Python 3.9.7; Waskom, 2021).

331 In order to answer the question whether or not lip movements enhance neural tracking, a control
332 for acoustic features is needed. This is particularly important due to the intercorrelation of speech
333 features (Chandrasekaran et al., 2009; Daube et al., 2019). To investigate the individual benefit
334 of lip movements, we used the averaged prediction accuracies in the audiovisual fROI and
335 subtracted the acoustic model from the acoustic+lip model (for a general overview on control
336 approaches see Gillis et al., 2022). The resulting individual benefit of lip movements was
337 expressed as percentage change (see Figure 2C).

338 *Statistical analysis and Bayesian modeling*

339 All frequentist statistical tests were conducted with built-in functions from eelbrain and the
340 statistical package pingouin version 0.5.2 (running on Python 3.9.7; Vallat, 2018). The three
341 behavioral measures (performance, difficulty, and motivation; Figure 1B) were statistically
342 compared between the two conditions (single speaker and multi speaker) using a Wilcoxon
343 signed-rank test and the matched-pairs rank-biserial correlation r_C was reported as effect size
344 (King et al., 2018).

345 The TRFs corresponding to the three stimulus features (spectrogram, acoustic onsets and lip
346 movements; Figure 2A), were tested for statistical difference between the two conditions using a
347 cluster-based permutation test with threshold-free cluster enhancement (TFCE; dependent
348 samples t-test, 10000 randomizations, Maris & Oostenveld, 2007; Smith & Nichols, 2009). Due to
349 the previously mentioned TRF regression artifacts, the time window for the test was limited to -50
350 to 550 ms. Depending on the direction of the cluster, the maximum or minimum t -value was
351 reported and Cohen's d of the averaged temporal extent of the cluster was calculated.

352 We tested the non-averaged prediction accuracies in the acoustic and lip fROIs (Figure 2B) with
353 a cluster-based permutation test with TFCE (dependent samples t-test, 10000 randomizations).
354 According to the cluster's direction, the maximum or minimum t -value was reported, and Cohen's
355 d of the cluster's averaged spatial extent was calculated. Additionally, averaged prediction
356 accuracies in the acoustic and lip fROIs were statistically tested with a dependent-samples t-test,

357 and Cohen's d was reported as effect size. In the audiovisual fROI, the prediction accuracies and
358 benefit of lip movements (Figure 2C) were tested with a dependent-samples t-test, and Cohen's
359 d was reported as effect size. If the data were not normally distributed according to a Shapiro-
360 Wilk test, the Wilcoxon signed-rank test was used, and the matched-pairs rank-biserial correlation
361 r_C was reported as effect size. The distribution of the benefit of lip movements was assessed
362 using the bimodality coefficient (Freeman & Dale, 2013).

363 To investigate if neural tracking is predictive for behavior, we calculated Bayesian multilevel
364 models in R version 4.2.2 (R Core Team, 2022) with the Stan-based package brms version 2.18.4
365 (Bürkner, 2017; Carpenter et al., 2017). Neural tracking (i.e. the averaged prediction accuracies
366 within the respective fROI) was used to separately predict the three behavioral measures. A
367 random intercept was added for each participant to account for repeated measures (single
368 speaker and multi speaker). The models were fitted independently for the acoustic and lip models
369 (Figure 3). According to the Wilkinson notation (Wilkinson & Rogers, 1973), the general formula
370 was:

371
$$\text{behavioral measure} \sim 1 + \text{neural tracking} + (1 | \text{participant})$$

372 We wanted to test whether the individual benefit of lip movements to neural speech tracking (see
373 *Forward models*) yields any behavioral relevance. For this, we also used the behavioral data of
374 the otherwise unanalyzed conditions with a face mask (see *Stimuli and experimental design*). We
375 fitted Bayesian multilevel models with the individual benefit of lip movements to separately predict
376 the behavioral measures when the speaker wore a face mask or not (Figure 4). The general
377 formula was:

378
$$\text{behavioral measure} \sim 1 + \text{benefit of lip movements} + (1 | \text{participant})$$

379 Before doing so, we fitted control models to show the effect of the conditions on the behavioral
380 measures when the lips are occluded (see Supplementary Table 1). Additional control models to
381 test the effect of the benefit of lip movements on the behavioral data without a face mask were
382 also fitted (see Supplementary Table 2 for model fits). In all described models, a random intercept
383 was included for each participant to account for repeated measures (single speaker and multi
384 speaker).

385 Weakly or non-informative default priors of brms were used, whose influence on the results is
386 negligible (Bürkner, 2017, 2018). For model calculation, all numerical variables were z-scored,

387 and standardized regression coefficients (b) were reported with 89% credible intervals (CIs; i.e.
388 Bayesian uncertainty intervals, McElreath, 2020). In addition, we report posterior probabilities
389 ($PP_{b>0}$) with values closer to 100%, providing evidence that the effect is greater than zero, and
390 closer to 0% that the effect was reversed (i.e. smaller than zero). If the 89% CIs for an estimate
391 did not include zero and $PP_{b>0}$ was below 5.5% or above 94.5%, the effects were considered
392 statistically significant.

393 All models were fitted with a Student-t distribution, as indicated by graphical posterior predictive
394 checks, Pareto \hat{k} diagnostics (Vehtari, Simpson, et al., 2022) and leave-one-out crossvalidation
395 via loo version 2.5.1 (Vehtari et al., 2017; Vehtari, Gabry, et al., 2022). Common algorithm-
396 agnostic (Vehtari et al., 2021) and algorithm-specific diagnostics (Betancourt, 2018) showed that
397 all Bayesian multilevel models converged. For all relevant parameters, the convergence
398 diagnostic $\hat{R} < 1.01$ and effective sample size (ESS) > 400 indicated that there were no divergent
399 transitions. Figures were created with ggplot2 version 3.4.0 (Wickham, 2016) and ggdist version
400 3.2.0 (Kay, 2022). Unstandardized b 's were used for the fitted values of the models in Figures 3
401 and 4.

402 *Data and Code Availability*

403 Preprocessed data and code are publicly available at GitHub ([https://github.com/reispat/](https://github.com/reispat/av_speech_mask)
404 `av_speech_mask`).

405 **Results**

406 Twenty-nine participants listened to audiobooks with a corresponding video of the speaker and a
407 randomly occurring audio-only distractor. Source-localized MEG responses to acoustic features
408 (spectrogram and acoustic onsets) and lip movements were predicted using forward models
409 (TRFs). We compared the TRFs between the two conditions and evaluated neural tracking of the
410 acoustic features and lip movements. The individual benefit of lip movements was obtained by
411 controlling for acoustic features and was compared between conditions. Using Bayesian
412 multilevel modeling, we predicted the behavioral measures with neural tracking. We also probed
413 the individual benefit of lip movements for their behavioral relevance by predicting the behavioral
414 measures when the lips were occluded with a surgical face mask or not.

415 *Listening situations with multiple speakers are behaviorally more demanding*

416 Participants performed worse in the multi speaker condition ($M = 62.93\%$, $SD = 17.34\%$),
417 compared to the single speaker condition ($M = 73.52\%$, $SD = 9.71\%$; $W = 73.00$, $p = .003$, $r_C =$
418 0.64). In the multi speaker condition, subjective difficulty ratings were higher ($M = 3.67$, $SD = 0.82$)
419 than in the single speaker condition ($M = 2.47$, $SD = 0.71$; $W = 11.50$, $p = 9.00e^{-06}$, $r_C = -0.95$).
420 Motivation was rated higher in the single speaker condition ($M = 3.91$, $SD = 0.74$) compared to
421 the multi speaker condition ($M = 3.72$, $SD = 0.85$; $W = 29.00$, $p = .024$, $r_C = 0.62$). Overall,
422 behavioral data showed that in the multi speaker condition, participants performed worse,
423 reported the task to be more difficult and were less motivated (Figure 1B).

424 *Neural responses to lip movements are enhanced in a multi speaker setting*

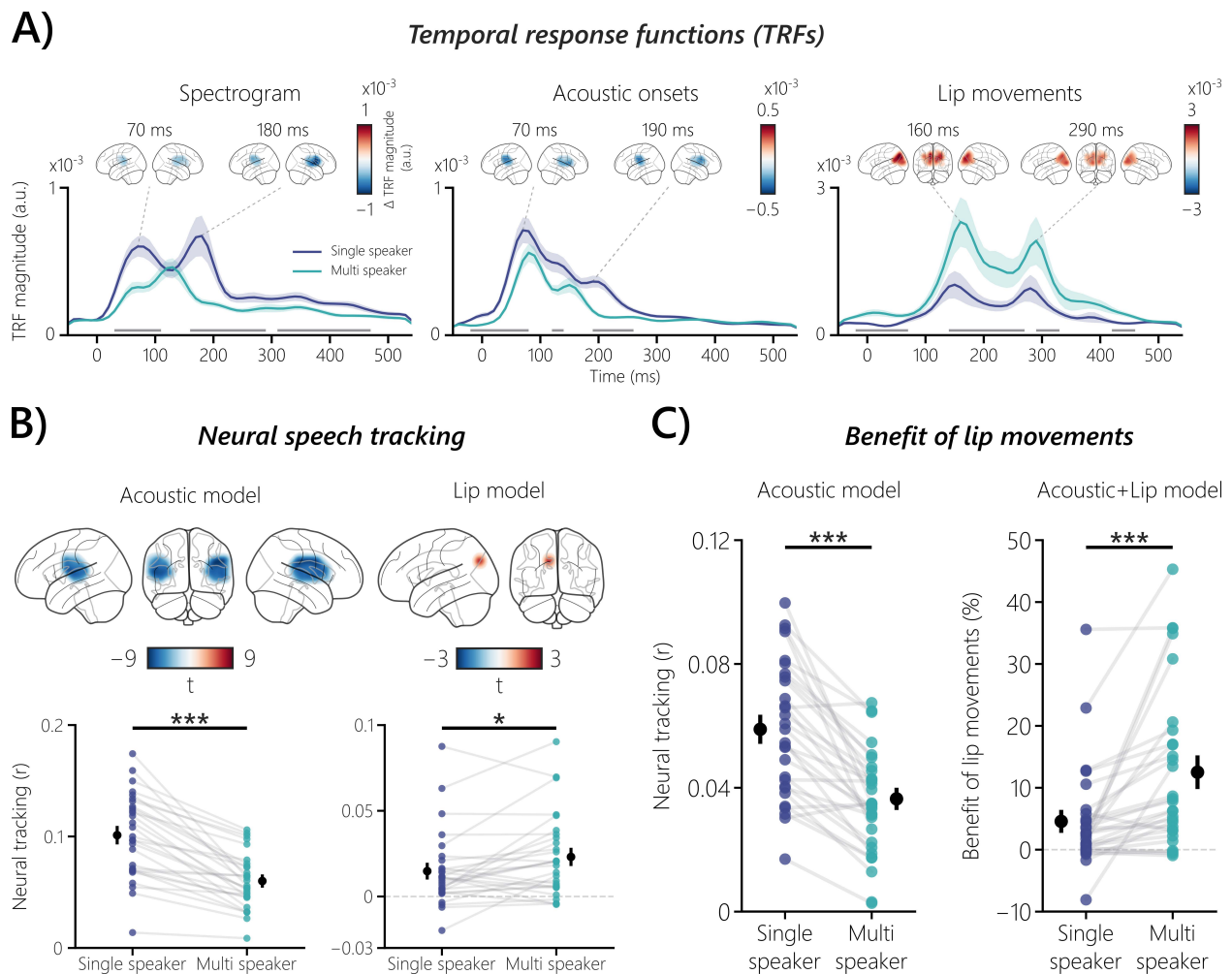
425 First, we analyzed the neural responses to acoustic and visual speech features by statistically
426 comparing the corresponding TRFs between the single- and multi speaker conditions within their
427 respective fROIs (Figure 2A). The spectrogram TRFs showed a significant difference between
428 conditions, with three clusters extending from early (30 to 110 ms; $t = -5.26$, $p = .0001$, $d = -0.81$),
429 middle (160 to 290 ms; $t = -3.78$, $p = .003$, $d = -1.00$) and late (310 to 470 ms; $t = -5.58$, $p = .0001$,
430 $d = -1.02$) time ranges. Grand-average TRF peaks are more pronounced in the single speaker
431 condition, with two peaks at 70 and 180 ms. While the first peak is also present in the multi speaker
432 condition, the second peak appeared 50 ms earlier than the single speaker setting. The latter
433 peak caused the largest differences in the magnitudes of the TRFs, which are most prominent in
434 the right hemisphere of the fROI.

435 The TRFs to acoustic onsets showed a significant difference between single- and multi speaker
436 speech, with three clusters extending from early (-20 to 80 ms; $t = -5.39$, $p < .001$, $d = -1.10$;
437 Figure 2A), mid (120 to 140 ms; $t = -4.54$, $p = .004$, $d = -1.43$) and mid-late (190 to 260 ms; $t = -$
438 6.11 , $p < .001$, $d = -1.13$) time windows. The TRFs showed two peaks at 70 and 190 ms in the
439 single speaker condition. Similar to the spectrogram TRFs, the first peak in the multi speaker
440 condition is at the same time point as in the single speaker condition and the second peak is 50
441 ms earlier. The magnitude differences across peaks and hemispheres are not substantially
442 different.

443 TRFs to lip movements show an opposite pattern to the TRFs to acoustic features, with stronger
444 processing in the multi speaker condition. Significant condition differences in the TRFs to lip
445 movements between single- and multi speaker speech were found, with four clusters extending

446 from early (-20 to 70 ms; $t = 4.41$, $p = .0005$, $d = 0.86$; Figure 2A), mid (140 to 270 ms; $t = 3.97$,
 447 $p = .001$, $d = 0.88$), mid-late (290 to 330 ms; $t = 3.34$, $p = .01$, $d = 0.91$) and late (420 to 460 ms;
 448 $t = 3.90$, $p = .002$, $d = 0.90$) time windows. The latencies of the peaks were later in general (160
 449 and 290 ms), as compared to the acoustic TRFs, which is also in line with the longer duration for
 450 a stimulus to reach the visual system (Thorpe et al., 1996; VanRullen & Thorpe, 2001). In the
 451 single speaker condition, they are delayed by 10 ms, and magnitude differences are most
 452 prominent in the first peak and left hemisphere.

453 Our initial analysis showed that neural responses to acoustic features are stronger when speech
 454 is clear. In contrast, neural responses to lip movements were enhanced in a multi speaker
 455 environment. The stronger processing of lip movements suggests a greater reliance on the lips
 456 of a speaker when speech is harder to understand.



457 **Figure 2.** *Neural responses to audiovisual speech features, neural speech tracking, and the benefit of lip*
458 *movements.* (A) The three plots show grand-averaged TRFs for the stimulus features in their respective
459 fROIs and the peak magnitude contrasts (multi speaker vs. single speaker) between the two conditions in
460 the involved sources. For the acoustic features, TRF magnitudes were generally enhanced when speech
461 was clear, with significant differences ranging from $p = .004$ to $p < .001$ ($d = -0.81$ to -1.43). In contrast, the
462 TRF to lip movements showed an enhanced magnitude in the multi speaker condition ($p = .01$ to $p = .0005$
463 and effect sizes from $d = 0.86$ to 0.91). The shaded areas of the respective conditions represent the
464 standard error of the mean (SEM). Gray bars indicate the temporal extent of significant differences ($p <$
465 $.05$) between the two conditions. (B) Neural speech tracking is shown for the non-averaged and averaged
466 fROIs of the acoustic and lip models. Acoustic neural tracking was higher in the single speaker condition,
467 with significant left- and right-hemispheric differences (both $p < .001$ with d from -1.30 to -1.47 ; averaged:
468 $p = 8.76e^{-09}$, $d = -1.30$). Lip movements were tracked higher in the multi speaker condition ($p = .037$, $d =$
469 0.51 ; averaged: $p = .026$, $r_C = 0.48$). In the averaged plots, the black dots represent the mean, and the
470 corresponding bars the SEM, of the respective condition. (C) In a combined acoustic and lip fROI, the
471 acoustic model showed higher neural tracking in the single speaker condition ($p = 7.68e^{-08}$, $d = 1.18$). The
472 benefit of lip movements was obtained by subtracting the acoustic model from the acoustic+lip model and
473 expressed as percentage change. Lip movements especially enhanced neural tracking in the multi speaker
474 condition ($p = .00003$, $r_C = 0.89$). Participants showed high interindividual variability with a visual benefit of
475 up to 45.37%, but also only a small benefit or no benefit at all. The black dots represent the mean, and the
476 corresponding bars the SEM, of the respective condition. $*p < .05$, $**p < .01$, $***p < .001$

477 *The cocktail party diametrically affects acoustic and visual neural speech tracking*

478 So far, the TRF results indicate a stronger neural response to lip movements and a weaker one
479 to acoustic features when there is more than one simultaneous speaker. We also wanted to
480 answer the question whether neural tracking of audiovisual speech features differs between the
481 single speaker and multi speaker conditions in their respective fROIs (Figure 2B; see Figure S1
482 for whole-brain neural tracking of the audiovisual speech features). Acoustic neural tracking in
483 the non-averaged acoustic fROI showed a significant condition difference in the left ($t = -8.04$, p
484 $< .001$, $d = -1.47$) and right ($t = -9.26$, $p < .001$, $d = -1.30$) hemispheres. Averaged acoustic neural
485 tracking was higher in the single speaker condition than in the multi speaker condition ($t(28) = -$
486 8.07 , $p = 8.76e^{-09}$, $d = -1.30$). Neural tracking of lip movements showed a significant condition
487 difference in the left hemisphere ($t = 3.83$, $p = .037$, $d = 0.51$; Figure 2B), with a focal inferior
488 parietal area involved. When averaging over sources, neural tracking was higher in the multi
489 speaker condition than in the single speaker condition ($W = 114.00$, $p = .026$, $r_C = 0.48$).

490 Overall, the results showed that neural tracking was enhanced for acoustic features when speech
491 is clear, and higher for lip movements when there are multiple speakers. This is in line with the
492 observed neural responses.

493 *Lip movements enhance neural speech tracking more in multi speaker situations*

494 When there are two speakers, we have so far demonstrated that lip movements are processed
495 more strongly and lead to higher neural tracking compared to one speaker. However, their unique
496 contribution to neural tracking is still unknown, due to the intercorrelation of speech features
497 (Chandrasekaran et al., 2009; Daube et al., 2019). To address this, we controlled for the acoustic
498 features so as to obtain the unique benefit of lip movements over and above acoustic speech
499 features. First, the acoustic model was evaluated in the audiovisual fROI (Figure 2C). Acoustic
500 neural tracking was higher in the single speaker condition than in the multi speaker condition
501 ($t(28) = -7.20, p = 7.68e^{-08}, d = 1.18$). The acoustic model served as a baseline and was subtracted
502 from a combined acoustic+lip model and expressed as percentage change. The obtained benefit
503 of lip movements was higher in the multi speaker condition than in the single speaker condition
504 ($W = 24.00, p = .00003, r_C = 0.89$). The benefit of lip movements showed high interindividual
505 variability and seemed to follow a bimodal distribution (Figure 2C), which was confirmed by a
506 bimodality coefficient of 0.68 (values > 0.555 indicate bimodality; Pfister et al., 2013).

507 These results strongly indicate that lip movements enhance neural tracking, especially in multi-
508 talker speech. However, substantial interindividual variability was observed, with participants
509 showing an individual benefit of lip movements of up to 45.37% in the multi speaker condition,
510 while others showed only a small benefit or no benefit at all. In the next steps, we will probe the
511 behavioral relevance of the benefit that lip movements provide to neural speech tracking by
512 depriving individuals of this source of information.

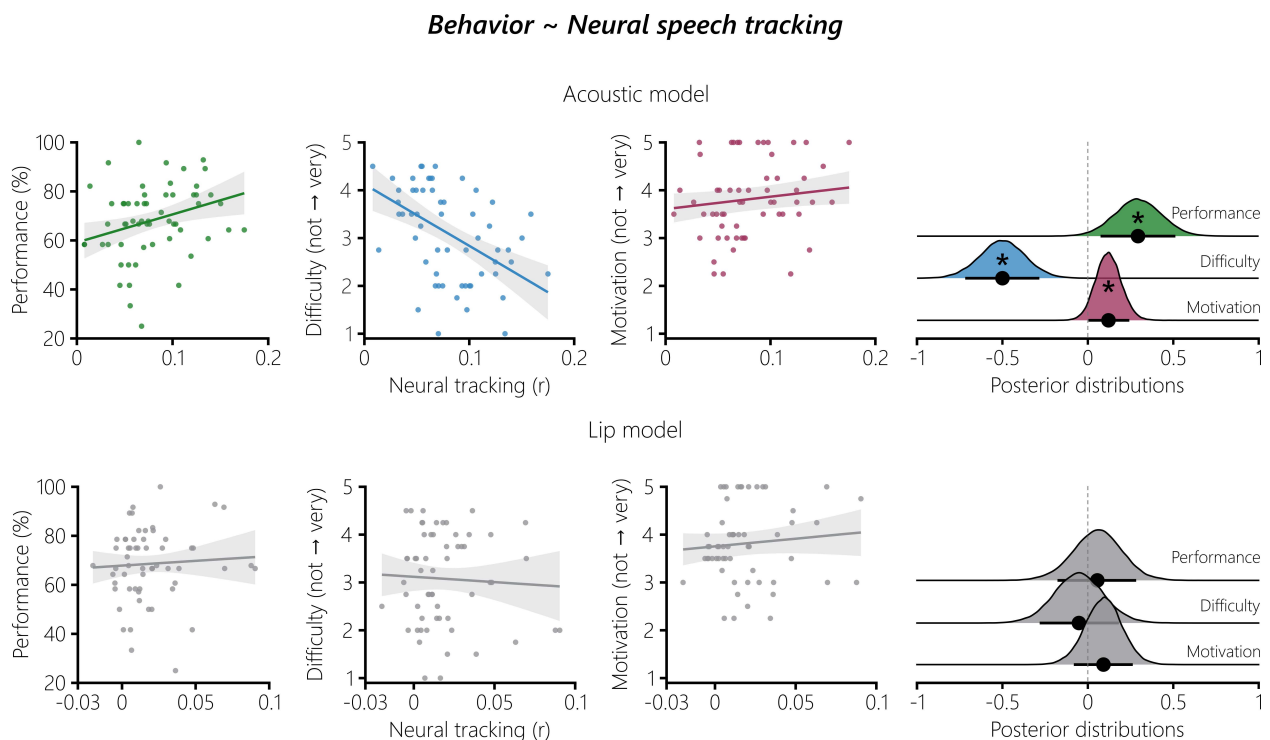
513 *Only acoustic neural speech tracking predicts behavior*

514 Having established that listening situations with two speakers affect neural tracking of acoustic
515 and visual speech features in a diametrical way, we were further interested if neural tracking is
516 able to predict the behavioral measures. We calculated Bayesian multilevel models to predict the
517 three behavioral measures (performance, difficulty and motivation; see Figure 1B) with the
518 averaged neural tracking of the acoustic and lip models (Figure 3). In the acoustic model, higher
519 neural tracking was linked to higher performance ($b = 0.29, 89\% \text{ CI} = [0.07, 0.51], \text{PP}_{b>0} =$
520 98.37%). Lower neural tracking predicted higher difficulty ratings ($b = -0.50, 89\% \text{ CI} = [-0.72, -$

521 0.29], $PP_{b>0} = 0.01\%$). When neural tracking was high, the motivation ratings were also higher (b
522 $= 0.12$, 89% CI = [0.004, 0.24], $PP_{b>0} = 95.05\%$).

523 Neural tracking of lip movements was not related to performance ($b = 0.06$, 89% CI = [-0.18, 0.28],
524 $PP_{b>0} = 65.61\%$; Figure 3). We also observed no evidence for an effect of the difficulty ($b = -0.05$,
525 89% CI = [-0.28, 0.18], $PP_{b>0} = 35.63\%$) or motivation ($b = 0.09$, 89% CI = [-0.08, 0.26], $PP_{b>0} =$
526 80.40%) ratings.

527 These results indicate that acoustic neural speech tracking predicts behavior: The higher the
528 neural speech tracking, the higher the performance and motivation ratings. Lower acoustic neural
529 speech tracking was linked to higher difficulty ratings. In contrast, neural speech tracking of lip
530 movements did not predict behavior.



531 **Figure 3. Relating behavior to neural speech tracking.** Bayesian multilevel models were fitted to predict the
532 behavioral measures with neural speech tracking. Higher acoustic neural speech tracking was linked to
533 higher performance, lower difficulty ratings and higher motivation ratings. No evidence for an effect was
534 observed for the neural tracking of lip movements. The shaded areas show the 89% CIs of the respective
535 model. The distributions on the right show the posterior draws of the three models. The black dots represent
536 the mean standardized regression coefficient b of the corresponding model. The corresponding bars show
537 the 89% CI. If zero was not part of the 89% CI, the effect was considered significant (*).

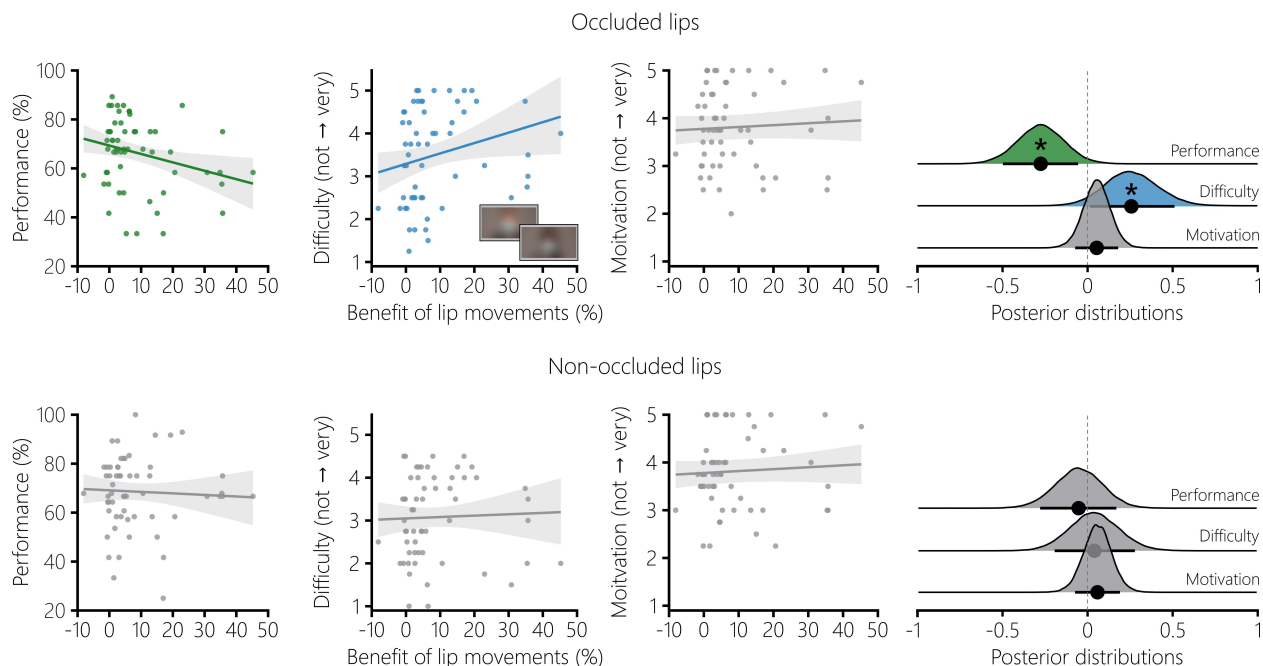
538 *Stronger benefit of lip movements predicts behavioral deterioration when lips are occluded*

539 Given the finding that lip movements enhance neural speech tracking (Figure 2C), we were
540 interested in whether this visual benefit is behaviorally relevant. To do so, we also used the
541 behavioral data from the otherwise unanalyzed conditions in which the mouth was occluded by a
542 surgical face mask (see Figure 4 for an example). Given that critical visual information is missing
543 in these conditions, individuals who show a strong benefit of lip movements on a neural level
544 should show poorer behavioral outcomes. An initial analysis showed that the effect of the
545 conditions with a surgical face mask on behavior followed the same pattern as those with non-
546 occluded lips (see Figure 1B), although with no effect on the motivation ratings. These control
547 models are reported in Supplementary Table 1.

548 While the effects on a solely behavioral level seem not to differ when the lips are occluded or not,
549 predicting the behavioral measures with the lip benefit showed the expected outcome (Figure 4):
550 Participants that had a higher benefit of lip movements in terms of neural tracking showed a
551 decline in performance ($b = -0.27$, 89% CI = [-0.49, -0.06], $PP_{b>0} = 2.21\%$) and reported the task
552 to be more difficult ($b = 0.25$, 89% CI = [0.01, 0.51], $PP_{b>0} = 95.41\%$). The motivation ratings did
553 not yield an effect ($b = 0.05$, 89% CI = [-0.07, 0.18], $PP_{b>0} = 76.14\%$).

554 Interestingly, we were not able to establish a link between the benefit of lip movements to the
555 behavioral data when the lips were not occluded (Figure 4; see Supplementary Table 2 for model
556 fits). Taken together, these findings support a behavioral relevance of the benefit of lip
557 movements. Individuals that benefit more from lip movements on a neural level performed worse
558 and reported the task to be more difficult when the mouth of the speaker was covered by a surgical
559 face mask.

Behavior ~ Benefit of lip movements



560 **Figure 4.** *Relating the benefit of lip movements to behavior.* The benefit of lip movements was used to
561 predict the behavioral measures when the lips are occluded or not. The values of the fitted Bayesian
562 multilevel models are shown with a depiction of the conditions in which the speakers wore a surgical face
563 mask. When the benefit of lip movements was high, performance was lower, and difficulty was reported
564 higher. No evidence for an effect was observed for the motivation rating. The behavioral measures when
565 the lips were not occluded were not linked to the benefit of lip movements. The shaded areas show the
566 89% CIs of the respective model. The distributions on the right show the posterior draws of the three
567 models. The black dots represent the mean standardized regression coefficient b of the corresponding
568 model. The corresponding bars show the 89% CI. If zero was not part of the 89% CI, the effect was
569 considered significant (*). *Speakers have been blurred due to a bioRxiv policy on the inclusion of faces.*

570 Discussion

571 Neural speech tracking is widely used to study the neural processing of continuous speech,
572 though primarily with audio-only stimuli (Brodbeck, Hong, et al., 2018; Chalas et al., 2022;
573 Di Liberto et al., 2015; Keitel et al., 2018). Recent studies have used audiovisual speech settings,
574 but without directly modeling the visual speech features (Crosse, Liberto, et al., 2016; Golumbic
575 et al., 2013) or not incorporating their temporal dynamics due to the use of frequency-based
576 methods (Aller et al., 2022; Bröhl et al., 2022; Park et al., 2016). Here, we show, for the first time,
577 the temporal dynamics and cortical origins of TRFs obtained from lip movements in an audiovisual

578 setting with one or two speakers. Using these neural responses, we demonstrate that the neural
579 tracking of lip movements is enhanced in a multi speaker situation compared to a single speaker.
580 When controlling for acoustic speech features, we show that the obtained benefit of lip
581 movements is enhanced in the multi speaker condition, although with high interindividual
582 variability. Using Bayesian modeling, we demonstrate that acoustic neural speech tracking
583 predicts the behavioral measures. Furthermore, individuals who displayed a higher benefit of lip
584 movements showed a stronger behavioral decline when the mouth was occluded with a surgical
585 face mask. Our findings show that individuals vary highly in their visual speech benefit and provide
586 new insights into the behavioral relevance of neural speech tracking.

587 *Neural responses to audiovisual speech*

588 Similar to Brodbeck, Hong, et al. (2018), neural responses to acoustic features in the two-speaker
589 paradigm were generally weaker. The TRFs to lip movements showed an opposite pattern, with
590 an enhanced magnitude in the multi speaker condition (Figure 2A), and with substantially later
591 peaks compared to the TRF to acoustic features. This is in line with Bourguignon et al. (2020),
592 where initial TRF peaks at 115 and 159 ms were shown from two significant sources, overlapping
593 with our involved parietal and occipital sources (see Figure 1C). However, the TRFs in their work
594 were modeled to lip movements from silent videos, which precludes a comparison between
595 different listening situations. Our findings also strengthen the argument that TRFs to visual speech
596 are qualitatively different from TRFs to acoustic speech (for coherence, see Park et al., 2016),
597 despite the high intercorrelation of speech features (Chandrasekaran et al., 2009).

598 *Neural tracking of audiovisual speech*

599 Based on the source-localized neural tracking, we determined fROIs via a data-driven approach
600 – separately for the acoustic features and lip movements (see Figure 1C). The fROIs for the
601 acoustic speech features involved sources along temporal, parietal and posterior frontal regions,
602 covering regions that are related to speech perception (Franken et al., 2022). Previous studies
603 source-localized TRFs in audio-only settings, though commonly restricting the analysis to
604 temporal regions (e.g. Brodbeck, Hong, et al., 2018; Kulasingham et al., 2020). The fROIs for the
605 lip movements involved parietal and occipital regions, in line with previous studies that source-
606 localized the neural tracking of lip movements (Aller et al., 2022; Bourguignon et al., 2020;
607 Hauswald et al., 2018). Similar to Park et al. (2016), we also observed neural tracking of lip
608 movements in temporal regions (see Figure S1), but with less involvement of the primary visual
609 cortex and prominent only in the single speaker condition. Due to our approach of defining our

610 fROIs based on the multi speaker condition, we removed any involvement of auditory regions in
611 the lip fROIs. In contrast to Park et al. (2016), we did not observe neural tracking of lip movements
612 in motor regions, resulting in no involvement of related sources in the lip fROIs.

613 When analyzing neural speech tracking in the acoustic fROIs, we showed a large effect with
614 enhanced tracking in the single speaker condition compared to the multi speaker condition (Figure
615 2B). We did not find a previous study that showed such a statistical contrast, which could be due
616 to the general focus on neural tracking of attended versus unattended speech, especially to
617 decode auditory attention (e.g. Ciccarelli et al., 2019; Geirnaert et al., 2021; Mirkovic et al., 2015;
618 J. A. O'Sullivan et al., 2015; Schäfer et al., 2018). On a group level, the neural tracking of lip
619 movements showed an enhancement in the multi speaker condition (Figure 2B). When comparing
620 the involved sources of the corresponding lip fROI, we found a medium effect in the left superior
621 parietal cortex. This is well in line with Park et al. (2016), showing an effect in left occipital and
622 parietal cortex when comparing two similar conditions to our design ("AV congruent vs. All
623 congruent"), although after partializing out auditory-related coherence. When we averaged the
624 neural tracking of lip movements, we observed interesting patterns, with participants showing no
625 meaningful neural tracking (i.e. close to zero or negative correlations) when there was one
626 speaker, but when speech became challenging, their neural tracking reached positive values.
627 Notably, this pattern was reversed for some participants, suggesting that not all of them used the
628 lip movements in the same manner. To investigate this further, eye tracking should be used to
629 identify which face regions participants fixated when attending audiovisual speech (e.g. Rennig &
630 Beauchamp, 2018) or to additionally incorporate a recently proposed phenomenon termed "ocular
631 speech tracking" (Gehmacher et al., 2023). Altogether, this is the first time that neural tracking of
632 lip movements has been quantified in the context of TRFs, although with substantially smaller
633 correlations as compared to acoustic speech tracking. Other algorithms, such as ridge regression,
634 could, in principle, yield higher values due to their optimization towards maximizing neural tracking
635 values (for a comparison of algorithms, see Kulasingham & Simon, 2022).

636 *Benefit of lip movements*

637 We first compared the neural tracking of audiovisual speech between single speaker and multi
638 speaker conditions in an isolated manner. Due to the aforementioned inter-correlation of speech
639 features (Chandrasekaran et al., 2009; Daube et al., 2019), this approach could not rule out any
640 acoustic contributions to the neural tracking of lip movements or vice versa. To reveal the unique
641 benefit of lip movements and to incorporate regions that are part of models of audiovisual speech

642 perception (Bernstein & Liebenthal, 2014) and multisensory integration (Pelle & Sommers,
643 2015), we combined both fROIs and controlled for acoustic speech features. Within the TRF
644 framework, we provide first evidence that lip movements enhance acoustic-controlled neural
645 speech tracking (Figure 2C). A general enhancement was observed for both single- and multi
646 speaker speech, which is in line with behavioral findings that visual speech features enhance
647 intelligibility under clear speech conditions as well (Blackburn et al., 2019; Stacey et al., 2016).
648 When comparing the two conditions, we observed a large effect, showing a higher benefit of lip
649 movements in the multi speaker condition. Our findings are also well in line with a previous study
650 (Park et al., 2016) that used partial coherence to remove auditory-related contributions, showing
651 higher coherence in a challenging audiovisual speech situation compared to a condition where
652 the audiovisual input was congruent.

653 Analogous to behavioral findings in Aller et al. (2022), the benefit of lip movements showed high
654 interindividual variability (see Figure 2C) and followed a bimodal distribution. Some individuals
655 benefited massively from lip movements, while others showed only a small benefit or none at all.
656 Interestingly, one individual even showed a negative influence when adding lip movements to the
657 acoustic model when there was only one speaker. As soon as speech became challenging, that
658 individual benefited from the lip information. Overall, these findings are in line with the beneficial
659 effects of visual speech when listening is challenging (e.g. Grant & Seitz, 2000; Remez, 2012;
660 Ross et al., 2007; Sumbly & Pollack, 1954). Given our moderate sample size, we refrained from
661 conducting further analysis by defining groups of individuals who showed a higher or lower benefit
662 of lip movements. Future studies should include more participants, as well as hearing-impaired
663 populations. A recent study that used neural tracking showed an increased audiovisual speech
664 benefit when speech was noisy (Puschmann et al., 2019). This could also provide a clearer picture
665 of how individuals benefit from lip movements in terms of neural tracking. Previous studies used
666 only the acoustic envelope to investigate the benefit of visual speech features on neural speech
667 tracking (Crosse, Liberto, et al., 2016; Golombic et al., 2013). Here, we also incorporated lip
668 movements to provide a more complete picture of the unique benefit of visual speech features in
669 audiovisual settings with naturalistic stimuli (Hamilton & Huth, 2020; A. E. O'Sullivan et al., 2019).

670 *Predicting behavior with neural tracking*

671 Our initial analysis of the behavioral measures suggests a higher cognitive demand when speech
672 was challenging (Figure 1B). Participants displayed lower task performance, higher difficulty
673 ratings and lower motivation ratings when more than one speaker was involved (Figure 1B). The

674 influence of challenging speech is also reflected in the findings of neural speech tracking (Figure
675 2B). Building on these results, we used Bayesian multilevel modeling to establish a link between
676 neural speech tracking and behavior (Figure 3). Higher acoustic neural tracking is related to
677 higher task performance, a finding also reported in a study that used vocoded speech (Chen et
678 al., 2023). We also show that higher acoustic neural tracking is related to lower difficulty ratings.
679 This is in line with a study that showed a positive relationship between speech intelligibility ratings
680 and acoustic neural tracking, though using speech-in-noise (Ding & Simon, 2013). Higher
681 motivation ratings were associated with higher acoustic neural tracking – in contrast to Schubert
682 et al. (2023) – showing no relationship between the two measures. We were not able to establish
683 any link between the neural tracking of lip movements and the behavioral measures. It is important
684 to note here that the analyzed neural tracking of lip movements was not yet controlled for speech
685 acoustics (Gillis et al., 2022), which could confound any relationship with behavior. A recent MEG
686 study impressively showed that the neural tracking of acoustic speech features can explain
687 cortical responses to higher-order linguistic features, such as phoneme onsets (Daube et al.,
688 2019), emphasizing the importance of controlling acoustics (see also Gillis et al., 2021).

689 The COVID-19 pandemic established the use of face masks on a global scale (Feng et al., 2020).
690 However, it has been demonstrated that covering the mouth has adverse effects on behavioral
691 measures, such as speech perception (e.g. Rahne et al., 2021). On a neural level, Haider et al.
692 (2022) showed that surgical face masks impair the neural tracking of acoustic and higher-order
693 segmentational speech features. However, the consequences of an absence of visual speech
694 were not analyzed in this study. Here, we establish a relationship between behavioral measures
695 and the individual benefit of visual speech on neural tracking. When the speaker wore a surgical
696 face mask, individuals that benefit more from lip movements displayed lower task performance
697 and higher difficulty ratings. Strikingly, no effect was found when the speaker did not wear a
698 surgical face mask. Overall, our results suggest that individuals who use lip movements more
699 effectively show behavioral deterioration when visual speech is absent. However, further studies
700 with larger sample sizes are needed to disentangle the potential influence of experimental
701 conditions on this relationship, e.g. using Bayesian mediation analysis (Nuijten et al., 2015; Yuan
702 & MacKinnon, 2009).

703 *Conclusion*

704 The current study provides first evidence for the substantial interindividual variability in the neural
705 tracking of lip movements and its relationship to behavior. First, we show that neural responses

706 to lip movements are more pronounced when speech is challenging, compared to when speech
707 is clear. We show that lip movements effectively enhance neural speech tracking in brain regions
708 related to audiovisual speech, with high interindividual variability. Furthermore, we demonstrate
709 that this individual visual benefit is behaviorally relevant. Individuals that benefit more from lip
710 movements have a lower task performance and rate the task to be more difficult when the speaker
711 wears a surgical face mask. Remarkably, this relationship is completely absent when the speaker
712 did not wear a mask. Our results provide new insights into the individual differences in the neural
713 tracking of lip movements and offer potential implications for future clinical and audiological
714 settings to objectively assess audiovisual speech perception.

715 **Acknowledgments**

716 P.R. is supported by the Austrian Science Fund (FWF; Doctoral College "Imaging the Mind"; W
717 1233-B), as well as N.S. ("Audiovisual speech entrainment in deafness"; P31230) and C.H.
718 ("Impact of face masks on speech comprehension"; P34237). P.R. is also supported by the
719 Austrian Research Promotion Agency (FFG; BRIDGE 1 project "SmartCIs"; 871232). M.G. is
720 supported by a Strategic Basic research grant by the Research Foundation Flanders (FWO, Grant
721 No. 1SA0620N). J.V. is supported by a postdoctoral grant provided by the FWO (Grant No.
722 1290821). The authors would like to thank Juliane Schubert for stimulus recordings and Sarah
723 Danböck for her helpful methodological input.

724 **Author Contributions**

725 P.R. analyzed the data, created the figures and wrote the manuscript. M.G. and J.V. analyzed the
726 data and edited the manuscript. N.S. and T.H. provided input on data analysis and edited the
727 manuscript. C.H. designed the study, collected the original dataset and edited the manuscript.
728 A.H. designed the study and edited the manuscript. K.S. edited the manuscript. T.F. supervised
729 the project and edited the manuscript. N.W. acquired the funding, supervised the project and
730 edited the manuscript.

731 **Conflict of interest statement**

732 K.S. is an employee of MED-EL GmbH. All other authors declare no competing interests.

733 **References**

- 734 Akalin-Acar, Z., & Gençer, N. G. (2004). An advanced boundary element method (BEM)
735 implementation for the forward problem of electromagnetic source imaging. *Physics in*
736 *Medicine & Biology*, 49(21), 5011. <https://doi.org/10.1088/0031-9155/49/21/012>
- 737 Aller, M., Økland, H. S., MacGregor, L. J., Blank, H., & Davis, M. H. (2022). Differential auditory
738 and visual phase-locking are observed during audio-visual benefit and silent lip-reading
739 for speech perception. *Journal of Neuroscience*, 42(31), 6108–6120.
740 <https://doi.org/10.1523/JNEUROSCI.2476-21.2022>
- 741 Bell, A. J., & Sejnowski, T. J. (1995). An Information-Maximization Approach to Blind Separation
742 and Blind Deconvolution. *Neural Computation*, 7(6), 1129–1159.
743 <https://doi.org/10.1162/neco.1995.7.6.1129>
- 744 Bernstein, L. E., & Liebenthal, E. (2014). Neural pathways for visual speech perception.
745 *Frontiers in Neuroscience*, 8.
746 <https://www.frontiersin.org/article/10.3389/fnins.2014.00386>
- 747 Besl, P. J., & McKay, N. D. (1992). A method for registration of 3-D shapes. *IEEE Transactions*
748 *on Pattern Analysis and Machine Intelligence*, 14(2), 239–256.
749 <https://doi.org/10.1109/34.121791>
- 750 Betancourt, M. (2018). *A Conceptual Introduction to Hamiltonian Monte Carlo*
751 (arXiv:1701.02434). arXiv. <https://doi.org/10.48550/arXiv.1701.02434>
- 752 Biesmans, W., Das, N., Francart, T., & Bertrand, A. (2017). Auditory-Inspired Speech Envelope
753 Extraction Methods for Improved EEG-Based Auditory Attention Detection in a Cocktail
754 Party Scenario. *IEEE Transactions on Neural Systems and Rehabilitation Engineering*,
755 25(5), 402–412. <https://doi.org/10.1109/TNSRE.2016.2571900>

- 756 Blackburn, C. L., Kitterick, P. T., Jones, G., Sumner, C. J., & Stacey, P. C. (2019). Visual
757 Speech Benefit in Clear and Degraded Speech Depends on the Auditory Intelligibility of
758 the Talker and the Number of Background Talkers. *Trends in Hearing*, 23.
759 <https://doi.org/10.1177/2331216519837866>
- 760 Boersma, P. (2001). Praat, a system for doing phonetics by computer. *Glott. Int.*, 5(9), 341–345.
- 761 Bourguignon, M., Baart, M., Kapnoula, E. C., & Molinaro, N. (2020). Lip-Reading Enables the
762 Brain to Synthesize Auditory Features of Unknown Silent Speech. *Journal of*
763 *Neuroscience*, 40(5), 1053–1065. <https://doi.org/10.1523/JNEUROSCI.1101-19.2019>
- 764 Brainard, D. H. (1997). The Psychophysics Toolbox. *Spatial Vision*, 10(4), 433–436.
765 <https://doi.org/10.1163/156856897X00357>
- 766 Brodbeck, C., Das, P., Gillis, M., Kulasingham, J. P., Bhattasali, S., Gaston, P., Resnik, P., &
767 Simon, J. Z. (2022). *Eelbrain: A Python toolkit for time-continuous analysis with temporal*
768 *response functions*. bioRxiv. <https://doi.org/10.1101/2021.08.01.454687>
- 769 Brodbeck, C., Hong, L. E., & Simon, J. Z. (2018). Rapid Transformation from Auditory to
770 Linguistic Representations of Continuous Speech. *Current Biology*, 28(24), 3976-
771 3983.e5. <https://doi.org/10.1016/j.cub.2018.10.042>
- 772 Brodbeck, C., Jiao, A., Hong, L. E., & Simon, J. Z. (2020). Neural speech restoration at the
773 cocktail party: Auditory cortex recovers masked speech of both attended and ignored
774 speakers. *PLOS Biology*, 18(10), e3000883.
775 <https://doi.org/10.1371/journal.pbio.3000883>
- 776 Brodbeck, C., Presacco, A., & Simon, J. Z. (2018). Neural source dynamics of brain responses
777 to continuous stimuli: Speech processing from acoustics to comprehension.
778 *NeuroImage*, 172, 162–174. <https://doi.org/10.1016/j.neuroimage.2018.01.042>
- 779 Brodbeck, C., & Simon, J. Z. (2020). Continuous speech processing. *Current Opinion in*
780 *Physiology*, 18, 25–31. <https://doi.org/10.1016/j.cophys.2020.07.014>

- 781 Broderick, M. P., Anderson, A. J., Di Liberto, G. M., Crosse, M. J., & Lalor, E. C. (2018).
782 Electrophysiological Correlates of Semantic Dissimilarity Reflect the Comprehension of
783 Natural, Narrative Speech. *Current Biology*, 28(5), 803-809.e3.
784 <https://doi.org/10.1016/j.cub.2018.01.080>
- 785 Bröhl, F., Keitel, A., & Kayser, C. (2022). MEG Activity in Visual and Auditory Cortices
786 Represents Acoustic Speech-Related Information during Silent Lip Reading. *ENeuro*,
787 9(3). <https://doi.org/10.1523/ENEURO.0209-22.2022>
- 788 Brown, V. A., Van Engen, K. J., & Peelle, J. E. (2021). Face mask type affects audiovisual
789 speech intelligibility and subjective listening effort in young and older adults. *Cognitive*
790 *Research: Principles and Implications*, 6(1), 49. [https://doi.org/10.1186/s41235-021-](https://doi.org/10.1186/s41235-021-00314-0)
791 [00314-0](https://doi.org/10.1186/s41235-021-00314-0)
- 792 Bürkner, P.-C. (2017). brms: An R Package for Bayesian Multilevel Models Using Stan. *Journal*
793 *of Statistical Software*, 80, 1–28. <https://doi.org/10.18637/jss.v080.i01>
- 794 Bürkner, P.-C. (2018). Advanced Bayesian Multilevel Modeling with the R Package brms. *The R*
795 *Journal*, 10(1), 395–411.
- 796 Carpenter, B., Gelman, A., Hoffman, M. D., Lee, D., Goodrich, B., Betancourt, M., Brubaker, M.,
797 Guo, J., Li, P., & Riddell, A. (2017). Stan: A Probabilistic Programming Language.
798 *Journal of Statistical Software*, 76, 1–32. <https://doi.org/10.18637/jss.v076.i01>
- 799 Chalas, N., Daube, C., Kluger, D. S., Abbasi, O., Nitsch, R., & Gross, J. (2022). Multivariate
800 analysis of speech envelope tracking reveals coupling beyond auditory cortex.
801 *NeuroImage*, 258, 119395. <https://doi.org/10.1016/j.neuroimage.2022.119395>
- 802 Chandrasekaran, C., Trubanova, A., Stillitano, S., Caplier, A., & Ghazanfar, A. A. (2009). The
803 Natural Statistics of Audiovisual Speech. *PLOS Computational Biology*, 5(7), e1000436.
804 <https://doi.org/10.1371/journal.pcbi.1000436>

- 805 Chen, Y.-P., Schmidt, F., Keitel, A., Rösch, S., Hauswald, A., & Weisz, N. (2023). Speech
806 intelligibility changes the temporal evolution of neural speech tracking. *NeuroImage*, *268*,
807 119894. <https://doi.org/10.1016/j.neuroimage.2023.119894>
- 808 Cherry, E. C. (1953). Some Experiments on the Recognition of Speech, with One and with Two
809 Ears. *The Journal of the Acoustical Society of America*, *25*(5), 975–979.
810 <https://doi.org/10.1121/1.1907229>
- 811 Chu, D. K., Akl, E. A., Duda, S., Solo, K., Yaacoub, S., Schünemann, H. J., Chu, D. K., Akl, E.
812 A., El-harakeh, A., Bognanni, A., Lotfi, T., Loeb, M., Hajizadeh, A., Bak, A., Izcovich, A.,
813 Cuello-Garcia, C. A., Chen, C., Harris, D. J., Borowiack, E., ... Schünemann, H. J.
814 (2020). Physical distancing, face masks, and eye protection to prevent person-to-person
815 transmission of SARS-CoV-2 and COVID-19: A systematic review and meta-analysis.
816 *The Lancet*, *395*(10242), 1973–1987. [https://doi.org/10.1016/S0140-6736\(20\)31142-9](https://doi.org/10.1016/S0140-6736(20)31142-9)
- 817 Ciccarelli, G., Nolan, M., Perricone, J., Calamia, P. T., Haro, S., O’Sullivan, J., Mesgarani, N.,
818 Quatieri, T. F., & Smalt, C. J. (2019). Comparison of Two-Talker Attention Decoding
819 from EEG with Nonlinear Neural Networks and Linear Methods. *Scientific Reports*, *9*(1),
820 11538. <https://doi.org/10.1038/s41598-019-47795-0>
- 821 Corey, D. M., Dunlap, W. P., & Burke, M. J. (1998). Averaging Correlations: Expected Values
822 and Bias in Combined Pearson r s and Fisher’s z Transformations. *The Journal of*
823 *General Psychology*, *125*(3), 245–261. <https://doi.org/10.1080/00221309809595548>
- 824 Crosse, M. J., Butler, J. S., & Lalor, E. C. (2015). Congruent Visual Speech Enhances Cortical
825 Entrainment to Continuous Auditory Speech in Noise-Free Conditions. *Journal of*
826 *Neuroscience*, *35*(42), 14195–14204. <https://doi.org/10.1523/JNEUROSCI.1829-15.2015>
- 827 Crosse, M. J., Di Liberto, G. M., Bednar, A., & Lalor, E. C. (2016). The multivariate temporal
828 response function (mTRF) toolbox: A Matlab toolbox for relating neural signals to
829 continuous stimuli. *Frontiers in Human Neuroscience*, *10*.

- 830 <https://doi.org/10.3389/fnhum.2016.00604>
- 831 Crosse, M. J., Liberto, G. M. D., & Lalor, E. C. (2016). Eye Can Hear Clearly Now: Inverse
832 Effectiveness in Natural Audiovisual Speech Processing Relies on Long-Term
833 Crossmodal Temporal Integration. *Journal of Neuroscience*, 36(38), 9888–9895.
834 <https://doi.org/10.1523/JNEUROSCI.1396-16.2016>
- 835 Crosse, M. J., Zuk, N. J., Di Liberto, G. M., Nidiffer, A. R., Molholm, S., & Lalor, E. C. (2021).
836 Linear Modeling of Neurophysiological Responses to Speech and Other Continuous
837 Stimuli: Methodological Considerations for Applied Research. *Frontiers in Neuroscience*,
838 15, 1350. <https://doi.org/10.3389/fnins.2021.705621>
- 839 Das, P., Brodbeck, C., Simon, J. Z., & Babadi, B. (2020). Neuro-current response functions: A
840 unified approach to MEG source analysis under the continuous stimuli paradigm.
841 *NeuroImage*, 211, 116528. <https://doi.org/10.1016/j.neuroimage.2020.116528>
- 842 Daube, C., Ince, R. A. A., & Gross, J. (2019). Simple Acoustic Features Can Explain Phoneme-
843 Based Predictions of Cortical Responses to Speech. *Current Biology*, 29(12), 1924-
844 1937.e9. <https://doi.org/10.1016/j.cub.2019.04.067>
- 845 David, S. V., Mesgarani, N., & Shamma, S. A. (2007). Estimating sparse spectro-temporal
846 receptive fields with natural stimuli. *Network: Computation in Neural Systems*, 18(3),
847 191–212. <https://doi.org/10.1080/09548980701609235>
- 848 de Jong, N. H., & Wempe, T. (2009). Praat script to detect syllable nuclei and measure speech
849 rate automatically. *Behavior Research Methods*, 41(2), 385–390.
850 <https://doi.org/10.3758/BRM.41.2.385>
- 851 Delorme, A., & Makeig, S. (2004). EEGLAB: An open source toolbox for analysis of single-trial
852 EEG dynamics including independent component analysis. *Journal of Neuroscience*
853 *Methods*, 134(1), 9–21. <https://doi.org/10.1016/j.jneumeth.2003.10.009>

- 854 Desikan, R. S., Ségonne, F., Fischl, B., Quinn, B. T., Dickerson, B. C., Blacker, D., Buckner, R.
855 L., Dale, A. M., Maguire, R. P., Hyman, B. T., Albert, M. S., & Killiany, R. J. (2006). An
856 automated labeling system for subdividing the human cerebral cortex on MRI scans into
857 gyral based regions of interest. *NeuroImage*, 31(3), 968–980.
858 <https://doi.org/10.1016/j.neuroimage.2006.01.021>
- 859 Di Liberto, G. M., O’Sullivan, J. A., & Lalor, E. C. (2015). Low-Frequency Cortical Entrainment to
860 Speech Reflects Phoneme-Level Processing. *Current Biology*, 25(19), 2457–2465.
861 <https://doi.org/10.1016/j.cub.2015.08.030>
- 862 Ding, N., & Simon, J. Z. (2013). Adaptive Temporal Encoding Leads to a Background-
863 Insensitive Cortical Representation of Speech. *Journal of Neuroscience*, 33(13), 5728–
864 5735. <https://doi.org/10.1523/JNEUROSCI.5297-12.2013>
- 865 Erber, N. P. (1975). Auditory-Visual Perception of Speech. *Journal of Speech and Hearing*
866 *Disorders*, 40(4), 481–492. <https://doi.org/10.1044/jshd.4004.481>
- 867 Feng, S., Shen, C., Xia, N., Song, W., Fan, M., & Cowling, B. J. (2020). Rational use of face
868 masks in the COVID-19 pandemic. *The Lancet Respiratory Medicine*, 8(5), 434–436.
869 [https://doi.org/10.1016/S2213-2600\(20\)30134-X](https://doi.org/10.1016/S2213-2600(20)30134-X)
- 870 Fischl, B. (2012). FreeSurfer. *NeuroImage*, 62(2), 774–781.
871 <https://doi.org/10.1016/j.neuroimage.2012.01.021>
- 872 Fishbach, A., Nelken, I., & Yeshurun, Y. (2001). Auditory Edge Detection: A Neural Model for
873 Physiological and Psychoacoustical Responses to Amplitude Transients. *Journal of*
874 *Neurophysiology*, 85(6), 2303–2323. <https://doi.org/10.1152/jn.2001.85.6.2303>
- 875 Franken, M. K., Liu, B. C., & Ostry, D. J. (2022). Towards a somatosensory theory of speech
876 perception. *Journal of Neurophysiology*, 128(6), 1683–1695.
877 <https://doi.org/10.1152/jn.00381.2022>

- 878 Freeman, J. B., & Dale, R. (2013). Assessing bimodality to detect the presence of a dual
879 cognitive process. *Behavior Research Methods*, 45(1), 83–97.
880 <https://doi.org/10.3758/s13428-012-0225-x>
- 881 Gehmacher, Q., Schubert, J., Schmidt, F., Hartmann, T., Reisinger, P., Rösch, S., Schwarz, K.,
882 Popov, T., Chait, M., & Weisz, N. (2023). *Eye movements track prioritized auditory*
883 *features in selective attention to natural speech*. bioRxiv.
884 <https://doi.org/10.1101/2023.01.23.525171>
- 885 Geirnaert, S., Vandecappelle, S., Alickovic, E., de Cheveigne, A., Lalor, E., Meyer, B. T., Miran,
886 S., Francart, T., & Bertrand, A. (2021). Electroencephalography-Based Auditory
887 Attention Decoding: Toward Neurosteered Hearing Devices. *IEEE Signal Processing*
888 *Magazine*, 38(4), 89–102. <https://doi.org/10.1109/MSP.2021.3075932>
- 889 Gillis, M., Van Canneyt, J., Francart, T., & Vanthornhout, J. (2022). Neural tracking as a
890 diagnostic tool to assess the auditory pathway. *Hearing Research*, 426, 108607.
891 <https://doi.org/10.1016/j.heares.2022.108607>
- 892 Gillis, M., Vanthornhout, J., Simon, J. Z., Francart, T., & Brodbeck, C. (2021). Neural Markers of
893 Speech Comprehension: Measuring EEG Tracking of Linguistic Speech
894 Representations, Controlling the Speech Acoustics. *Journal of Neuroscience*, 41(50),
895 10316–10329. <https://doi.org/10.1523/JNEUROSCI.0812-21.2021>
- 896 Golumbic, E. Z., Cogan, G. B., Schroeder, C. E., & Poeppel, D. (2013). Visual Input Enhances
897 Selective Speech Envelope Tracking in Auditory Cortex at a “Cocktail Party.” *Journal of*
898 *Neuroscience*, 33(4), 1417–1426. <https://doi.org/10.1523/JNEUROSCI.3675-12.2013>
- 899 Gramfort, A., Luessi, M., Larson, E., Engemann, D. A., Strohmeier, D., Brodbeck, C.,
900 Parkkonen, L., & Hämäläinen, M. S. (2014). MNE software for processing MEG and
901 EEG data. *NeuroImage*, 86, 446–460. <https://doi.org/10.1016/j.neuroimage.2013.10.027>

- 902 Gramfort, A., Luessi, M., Larson, E., Engemann, D., Strohmeier, D., Brodbeck, C., Goj, R., Jas,
903 M., Brooks, T., Parkkonen, L., & Hämäläinen, M. (2013). MEG and EEG data analysis
904 with MNE-Python. *Frontiers in Neuroscience*, 7.
905 <https://www.frontiersin.org/articles/10.3389/fnins.2013.00267>
- 906 Grant, K. W., & Seitz, P.-F. (2000). The use of visible speech cues for improving auditory
907 detection of spoken sentences. *The Journal of the Acoustical Society of America*,
908 108(3), 1197–1208. <https://doi.org/10.1121/1.1288668>
- 909 Haider, C. L., Suess, N., Hauswald, A., Park, H., & Weisz, N. (2022). Masking of the mouth area
910 impairs reconstruction of acoustic speech features and higher-level segmentational
911 features in the presence of a distractor speaker. *NeuroImage*, 252, 119044.
912 <https://doi.org/10.1016/j.neuroimage.2022.119044>
- 913 Hämäläinen, M. S., & Ilmoniemi, R. J. (1994). Interpreting magnetic fields of the brain: Minimum
914 norm estimates. *Medical & Biological Engineering & Computing*, 32(1), 35–42.
915 <https://doi.org/10.1007/BF02512476>
- 916 Hamilton, L. S., & Huth, A. G. (2020). The revolution will not be controlled: Natural stimuli in
917 speech neuroscience. *Language, Cognition and Neuroscience*, 35(5), 573–582.
918 <https://doi.org/10.1080/23273798.2018.1499946>
- 919 Hartmann, T., & Weisz, N. (2020). An introduction to the Objective Psychophysics Toolbox
920 (o_ptb). *Frontiers in Psychology*, 11. <https://doi.org/10.3389/fpsyg.2020.585437>
- 921 Hauswald, A., Lithari, C., Collignon, O., Leonardelli, E., & Weisz, N. (2018). A Visual Cortical
922 Network for Deriving Phonological Information from Intelligible Lip Movements. *Current*
923 *Biology*, 28(9), 1453-1459.e3. <https://doi.org/10.1016/j.cub.2018.03.044>
- 924 Heeris, J. (2013). *Gammatone Filterbank Toolkit*. <https://github.com/detly/gammatone>
- 925 Houck, J. M., & Claus, E. D. (2020). A comparison of automated and manual co-registration for
926 magnetoencephalography. *PLOS ONE*, 15(4), e0232100.

- 927 <https://doi.org/10.1371/journal.pone.0232100>
- 928 Kay, M. (2022). *ggdist: Visualizations of distributions and uncertainty*. Zenodo.
- 929 <https://doi.org/10.5281/zenodo.6862765>
- 930 Keitel, A., Gross, J., & Kayser, C. (2018). Perceptually relevant speech tracking in auditory and
931 motor cortex reflects distinct linguistic features. *PLOS Biology*, 16(3), e2004473.
932 <https://doi.org/10.1371/journal.pbio.2004473>
- 933 King, B. M., Rosopa, P. J., & Minium, E. W. (2018). *Statistical Reasoning in the Behavioral*
934 *Sciences* (7th Edition). John Wiley & Sons.
- 935 Kleiner, M., Brainard, D., & Pelli, D. (2007). What's new in Psychtoolbox-3? *Perception*, 36, 1–
936 16.
- 937 Kulasingham, J. P., Brodbeck, C., Presacco, A., Kuchinsky, S. E., Anderson, S., & Simon, J. Z.
938 (2020). High gamma cortical processing of continuous speech in younger and older
939 listeners. *NeuroImage*, 222, 117291. <https://doi.org/10.1016/j.neuroimage.2020.117291>
- 940 Kulasingham, J. P., & Simon, J. Z. (2022). Algorithms for Estimating Time-Locked Neural
941 Response Components in Cortical Processing of Continuous Speech. *IEEE*
942 *Transactions on Biomedical Engineering*, 1–9.
943 <https://doi.org/10.1109/TBME.2022.3185005>
- 944 Lalor, E. C., Pearlmitter, B. A., Reilly, R. B., McDarby, G., & Foxe, J. J. (2006). The VESPA: A
945 method for the rapid estimation of a visual evoked potential. *NeuroImage*, 32(4), 1549–
946 1561. <https://doi.org/10.1016/j.neuroimage.2006.05.054>
- 947 Lalor, E. C., Power, A. J., Reilly, R. B., & Foxe, J. J. (2009). Resolving Precise Temporal
948 Processing Properties of the Auditory System Using Continuous Stimuli. *Journal of*
949 *Neurophysiology*, 102(1), 349–359. <https://doi.org/10.1152/jn.90896.2008>

- 950 Lin, F.-H., Witzel, T., Ahlfors, S. P., Stufflebeam, S. M., Belliveau, J. W., & Hämäläinen, M. S.
951 (2006). Assessing and improving the spatial accuracy in MEG source localization by
952 depth-weighted minimum-norm estimates. *NeuroImage*, 31(1), 160–171.
953 <https://doi.org/10.1016/j.neuroimage.2005.11.054>
- 954 Maris, E., & Oostenveld, R. (2007). Nonparametric statistical testing of EEG- and MEG-data.
955 *Journal of Neuroscience Methods*, 164(1), 177–190.
956 <https://doi.org/10.1016/j.jneumeth.2007.03.024>
- 957 McDermott, J. H. (2009). The cocktail party problem. *Current Biology*, 19(22), R1024–R1027.
958 <https://doi.org/10.1016/j.cub.2009.09.005>
- 959 McElreath, R. (2020). *Statistical Rethinking: A Bayesian Course with Examples in R and STAN*
960 (2nd ed.). Chapman and Hall/CRC. <https://doi.org/10.1201/9780429029608>
- 961 Meredith, M. A., & Stein, B. E. (1983). Interactions Among Converging Sensory Inputs in the
962 Superior Colliculus. *Science*, 221(4608), 389–391.
963 <https://doi.org/10.1126/science.6867718>
- 964 Mirkovic, B., Debener, S., Jaeger, M., & Vos, M. D. (2015). Decoding the attended speech
965 stream with multi-channel EEG: Implications for online, daily-life applications. *Journal of*
966 *Neural Engineering*, 12(4), 046007. <https://doi.org/10.1088/1741-2560/12/4/046007>
- 967 Nidiffer, A. R., Cao, C. Z., O'Sullivan, A., & Lalor, E. C. (2021). *A linguistic representation in the*
968 *visual system underlies successful lipreading*. bioRxiv.
969 <https://www.biorxiv.org/content/10.1101/2021.02.09.430299v1>
- 970 Nieto-Castanon, A., Ghosh, S. S., Tourville, J. A., & Guenther, F. H. (2003). Region of interest
971 based analysis of functional imaging data. *NeuroImage*, 19(4), 1303–1316.
972 [https://doi.org/10.1016/S1053-8119\(03\)00188-5](https://doi.org/10.1016/S1053-8119(03)00188-5)
- 973 Nuijten, M. B., Wetzels, R., Matzke, D., Dolan, C. V., & Wagenmakers, E.-J. (2015). A default
974 Bayesian hypothesis test for mediation. *Behavior Research Methods*, 47(1), 85–97.

- 975 <https://doi.org/10.3758/s13428-014-0470-2>
- 976 Obleser, J., & Kayser, C. (2019). Neural Entrainment and Attentional Selection in the Listening
977 Brain. *Trends in Cognitive Sciences*, 23(11), 913–926.
978 <https://doi.org/10.1016/j.tics.2019.08.004>
- 979 Oostenveld, R., Fries, P., Maris, E., & Schoffelen, J.-M. (2011). *FieldTrip: Open Source*
980 *Software for Advanced Analysis of MEG, EEG, and Invasive Electrophysiological Data*
981 [Research article]. *Computational Intelligence and Neuroscience*.
982 <https://doi.org/10.1155/2011/156869>
- 983 O’Sullivan, A. E., Lim, C. Y., & Lalor, E. C. (2019). Look at me when I’m talking to you: Selective
984 attention at a multisensory cocktail party can be decoded using stimulus reconstruction
985 and alpha power modulations. *European Journal of Neuroscience*, 50(8), 3282–3295.
986 <https://doi.org/10.1111/ejn.14425>
- 987 O’Sullivan, J. A., Power, A. J., Mesgarani, N., Rajaram, S., Foxe, J. J., Shinn-Cunningham, B.
988 G., Slaney, M., Shamma, S. A., & Lalor, E. C. (2015). Attentional Selection in a Cocktail
989 Party Environment Can Be Decoded from Single-Trial EEG. *Cerebral Cortex*, 25(7),
990 1697–1706. <https://doi.org/10.1093/cercor/bht355>
- 991 Park, H., Kayser, C., Thut, G., & Gross, J. (2016). Lip movements entrain the observers’ low-
992 frequency brain oscillations to facilitate speech intelligibility. *ELife*, 5, e14521.
993 <https://doi.org/10.7554/eLife.14521>
- 994 Peelle, J. E., & Sommers, M. S. (2015). Prediction and constraint in audiovisual speech
995 perception. *Cortex*, 68, 169–181. <https://doi.org/10.1016/j.cortex.2015.03.006>
- 996 Pelli, D. G. (1997). The VideoToolbox software for visual psychophysics: Transforming numbers
997 into movies. *Spatial Vision*, 10(4), 437–442. <https://doi.org/10.1163/156856897X00366>
- 998 Pfister, R., Schwarz, K., Janczyk, M., Dale, R., & Freeman, J. (2013). Good things peak in pairs:
999 A note on the bimodality coefficient. *Frontiers in Psychology*, 4.

- 1000 <https://www.frontiersin.org/articles/10.3389/fpsyg.2013.00700>
- 1001 Puschmann, S., Daeglau, M., Stropahl, M., Mirkovic, B., Rosemann, S., Thiel, C. M., &
1002 Debener, S. (2019). Hearing-impaired listeners show increased audiovisual benefit when
1003 listening to speech in noise. *NeuroImage*, 196, 261–268.
1004 <https://doi.org/10.1016/j.neuroimage.2019.04.017>
- 1005 R Core Team. (2022). *R: A Language and Environment for Statistical Computing*. R Foundation
1006 for Statistical Computing. <https://www.R-project.org/>
- 1007 Rahne, T., Fröhlich, L., Plontke, S., & Wagner, L. (2021). Influence of surgical and N95 face
1008 masks on speech perception and listening effort in noise. *PLOS ONE*, 16(7), e0253874.
1009 <https://doi.org/10.1371/journal.pone.0253874>
- 1010 Remez, R. E. (2012). Three puzzles of multimodal speech perception. In E. Vatikiotis-Bateson,
1011 G. Bailly, & P. Perrier (Eds.), *Audiovisual Speech Processing* (pp. 4–20). Cambridge
1012 University Press. <https://doi.org/10.1017/CBO9780511843891.003>
- 1013 Rennig, J., & Beauchamp, M. S. (2018). Free viewing of talking faces reveals mouth and eye
1014 preferring regions of the human superior temporal sulcus. *NeuroImage*, 183, 25–36.
1015 <https://doi.org/10.1016/j.neuroimage.2018.08.008>
- 1016 Ross, L. A., Molholm, S., Butler, J. S., Bene, V. A. D., & Foxe, J. J. (2022). Neural correlates of
1017 multisensory enhancement in audiovisual narrative speech perception: A fMRI
1018 investigation. *NeuroImage*, 263, 119598.
1019 <https://doi.org/10.1016/j.neuroimage.2022.119598>
- 1020 Ross, L. A., Saint-Amour, D., Leavitt, V. M., Javitt, D. C., & Foxe, J. J. (2007). Do You See What
1021 I Am Saying? Exploring Visual Enhancement of Speech Comprehension in Noisy
1022 Environments. *Cerebral Cortex*, 17(5), 1147–1153. <https://doi.org/10.1093/cercor/bhl024>

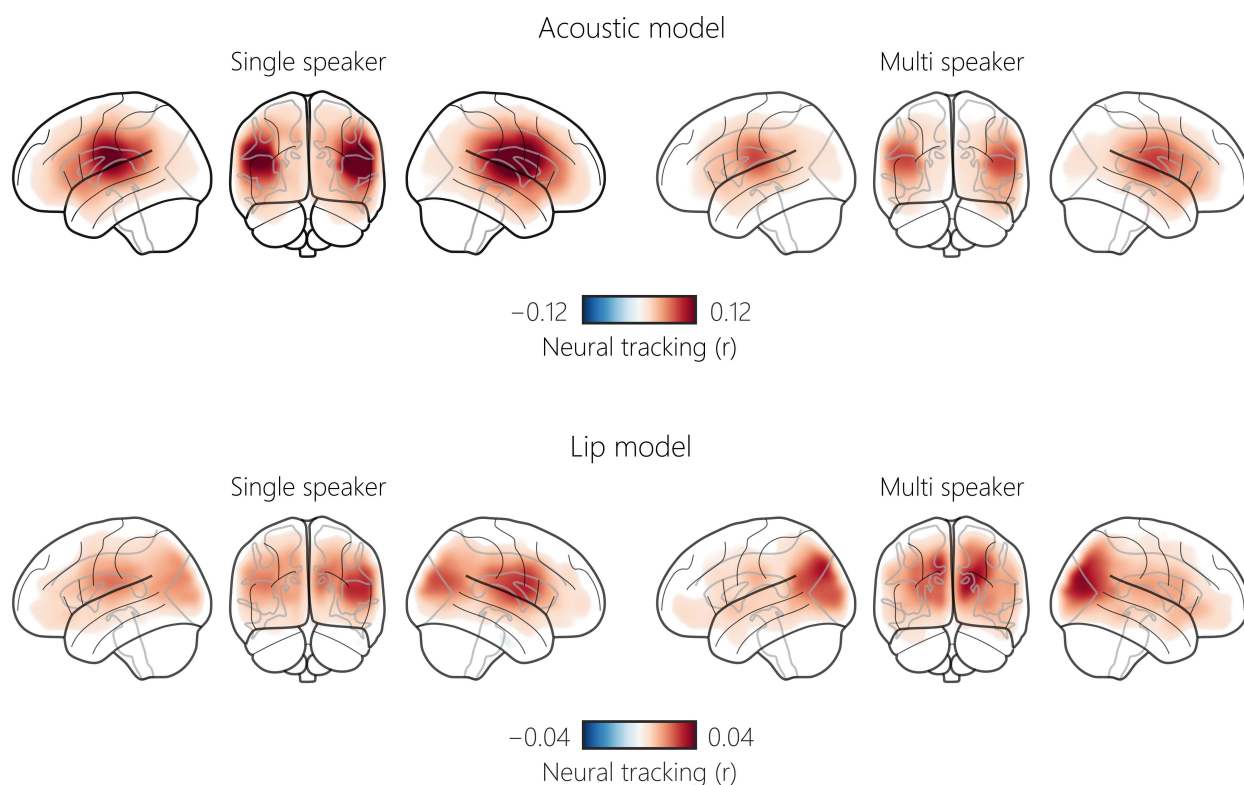
- 1023 Schäfer, P. J., Corona-Strauss, F. I., Hannemann, R., Hillyard, S. A., & Strauss, D. J. (2018).
1024 Testing the Limits of the Stimulus Reconstruction Approach: Auditory Attention Decoding
1025 in a Four-Speaker Free Field Environment. *Trends in Hearing*, 22.
1026 <https://doi.org/10.1177/2331216518816600>
- 1027 Schmitt, R., Meyer, M., & Giroud, N. (2022). Better speech-in-noise comprehension is
1028 associated with enhanced neural speech tracking in older adults with hearing
1029 impairment. *Cortex*, 151, 133–146. <https://doi.org/10.1016/j.cortex.2022.02.017>
- 1030 Schubert, J., Schmidt, F., Gehmacher, Q., Bresgen, A., & Weisz, N. (2023). Cortical speech
1031 tracking is related to individual prediction tendencies. *Cerebral Cortex*, bhac528.
1032 <https://doi.org/10.1093/cercor/bhac528>
- 1033 Slaney, M. (1998). Auditory toolbox. *Interval Research Corporation*, 10(1998), 1194.
- 1034 Smith, S. M., & Nichols, T. E. (2009). Threshold-free cluster enhancement: Addressing
1035 problems of smoothing, threshold dependence and localisation in cluster inference.
1036 *NeuroImage*, 44(1), 83–98. <https://doi.org/10.1016/j.neuroimage.2008.03.061>
- 1037 Stacey, P. C., Kitterick, P. T., Morris, S. D., & Sumner, C. J. (2016). The contribution of visual
1038 information to the perception of speech in noise with and without informative temporal
1039 fine structure. *Hearing Research*, 336, 17–28.
1040 <https://doi.org/10.1016/j.heares.2016.04.002>
- 1041 Suess, N., Hauswald, A., Reisinger, P., Rösch, S., Keitel, A., & Weisz, N. (2022). Cortical
1042 Tracking of Formant Modulations Derived from Silently Presented Lip Movements and
1043 Its Decline with Age. *Cerebral Cortex*, bhab518. <https://doi.org/10.1093/cercor/bhab518>
- 1044 Suess, N., Hauswald, A., Zehentner, V., Depireux, J., Herzog, G., Rösch, S., & Weisz, N.
1045 (2022). Influence of linguistic properties and hearing impairment on visual speech
1046 perception skills in the German language. *PLOS ONE*, 17(9), e0275585.
1047 <https://doi.org/10.1371/journal.pone.0275585>

- 1048 Sumbly, W. H., & Pollack, I. (1954). Visual Contribution to Speech Intelligibility in Noise. *The*
1049 *Journal of the Acoustical Society of America*, 26(2), 212–215.
1050 <https://doi.org/10.1121/1.1907309>
- 1051 Summerfield, Q., Bruce, V., Cowey, A., Ellis, A. W., & Perrett, D. I. (1992). Lipreading and
1052 audio-visual speech perception. *Philosophical Transactions of the Royal Society of*
1053 *London. Series B: Biological Sciences*, 335(1273), 71–78.
1054 <https://doi.org/10.1098/rstb.1992.0009>
- 1055 Suñer, C., Coma, E., Ouchi, D., Hermosilla, E., Baro, B., Rodríguez-Arias, M. À., Puig, J.,
1056 Clotet, B., Medina, M., & Mitjà, O. (2022). Association between two mass-gathering
1057 outdoor events and incidence of SARS-CoV-2 infections during the fifth wave of COVID-
1058 19 in north-east Spain: A population-based control-matched analysis. *The Lancet*
1059 *Regional Health - Europe*, 15, 100337. <https://doi.org/10.1016/j.lanepe.2022.100337>
- 1060 Taulu, S., & Kajola, M. (2005). Presentation of electromagnetic multichannel data: The signal
1061 space separation method. *Journal of Applied Physics*, 97(12), 124905.
1062 <https://doi.org/10.1063/1.1935742>
- 1063 Taulu, S., & Simola, J. (2006). Spatiotemporal signal space separation method for rejecting
1064 nearby interference in MEG measurements. *Physics in Medicine & Biology*, 51(7), 1759.
1065 <https://doi.org/10.1088/0031-9155/51/7/008>
- 1066 Thorpe, S., Fize, D., & Marlot, C. (1996). Speed of processing in the human visual system.
1067 *Nature*, 381(6582), 520–522. <https://doi.org/10.1038/381520a0>
- 1068 Vallat, R. (2018). Pingouin: Statistics in Python. *Journal of Open Source Software*, 3(31), 1026.
1069 <https://doi.org/10.21105/joss.01026>
- 1070 van de Rijt, L. P. H., Roye, A., Mylanus, E. A. M., van Opstal, A. J., & van Wanrooij, M. M.
1071 (2019). The Principle of Inverse Effectiveness in Audiovisual Speech Perception.
1072 *Frontiers in Human Neuroscience*, 13.

- 1073 <https://www.frontiersin.org/articles/10.3389/fnhum.2019.00335>
- 1074 VanRullen, R., & Thorpe, S. J. (2001). The Time Course of Visual Processing: From Early
1075 Perception to Decision-Making. *Journal of Cognitive Neuroscience*, 13(4), 454–461.
1076 <https://doi.org/10.1162/08989290152001880>
- 1077 Vanthornhout, J., Decruy, L., Wouters, J., Simon, J. Z., & Francart, T. (2018). Speech
1078 Intelligibility Predicted from Neural Entrainment of the Speech Envelope. *Journal of the*
1079 *Association for Research in Otolaryngology*, 19(2), 181–191.
1080 <https://doi.org/10.1007/s10162-018-0654-z>
- 1081 Vehtari, A., Gabry, J., Magnusson, M., Yao, Y., Bürkner, P.-C., Paananen, T., & Gelman, A.
1082 (2022). *loo: Efficient leave-one-out cross-validation and WAIC for Bayesian models*.
1083 <https://mc-stan.org/loo/>
- 1084 Vehtari, A., Gelman, A., & Gabry, J. (2017). Practical Bayesian model evaluation using leave-
1085 one-out cross-validation and WAIC. *Statistics and Computing*, 27(5), 1413–1432.
1086 <https://doi.org/10.1007/s11222-016-9696-4>
- 1087 Vehtari, A., Gelman, A., Simpson, D., Carpenter, B., & Bürkner, P.-C. (2021). Rank-
1088 Normalization, Folding, and Localization: An Improved $R^{\hat{}}$ for Assessing Convergence of
1089 MCMC (with Discussion). *Bayesian Analysis*, 16(2), 667–718. [https://doi.org/10.1214/20-](https://doi.org/10.1214/20-BA1221)
1090 [BA1221](https://doi.org/10.1214/20-BA1221)
- 1091 Vehtari, A., Simpson, D., Gelman, A., Yao, Y., & Gabry, J. (2022). *Pareto Smoothed Importance*
1092 *Sampling* (arXiv:1507.02646). arXiv. <https://doi.org/10.48550/arXiv.1507.02646>
- 1093 Virtanen, P., Gommers, R., Oliphant, T. E., Haberland, M., Reddy, T., Cournapeau, D.,
1094 Burovski, E., Peterson, P., Weckesser, W., Bright, J., van der Walt, S. J., Brett, M.,
1095 Wilson, J., Millman, K. J., Mayorov, N., Nelson, A. R. J., Jones, E., Kern, R., Larson, E.,
1096 ... van Mulbregt, P. (2020). SciPy 1.0: Fundamental algorithms for scientific computing
1097 in Python. *Nature Methods*, 17(3), Article 3. <https://doi.org/10.1038/s41592-019-0686-2>

- 1098 Waskom, M. L. (2021). seaborn: Statistical data visualization. *Journal of Open Source Software*,
1099 6(60), 3021. <https://doi.org/10.21105/joss.03021>
- 1100 Wickham, H. (2016). *ggplot2: Elegant Graphics for Data Analysis*. Springer-Verlag New York.
1101 <https://ggplot2.tidyverse.org>
- 1102 Wilkinson, G. N., & Rogers, C. E. (1973). Symbolic Description of Factorial Models for Analysis
1103 of Variance. *Journal of the Royal Statistical Society. Series C (Applied Statistics)*, 22(3),
1104 392–399. <https://doi.org/10.2307/2346786>
- 1105 Yuan, Y., & MacKinnon, D. P. (2009). Bayesian mediation analysis. *Psychological Methods*, 14,
1106 301–322. <https://doi.org/10.1037/a0016972>
- 1107 Zhang, L., & Du, Y. (2022). Lip movements enhance speech representations and effective
1108 connectivity in auditory dorsal stream. *NeuroImage*, 257, 119311.
1109 <https://doi.org/10.1016/j.neuroimage.2022.119311>

1110 **Supplementary Materials**



1111 **Figure S1.** Whole-brain neural tracking of the audiovisual speech features. Neural tracking (r) of all sources
 1112 is shown for the acoustic model (spectrogram and acoustic onsets) and the lip model (lip movements).

	Conditions		
	b	89% CI	PP _{$b>0$}
Performance (occluded lips)	-0.77	[-1.13, -0.41]*	0.07%*
Difficulty (occluded lips)	1.26	[1.04, 1.49]*	100%*
Motivation (occluded lips)	-0.11	[-0.27, 0.04]	11.11%

1113 **Supplementary Table 1.** Effects of conditions on behavior when the lips are occluded. The formula was:
 1114 $behavioral\ measure \sim 1 + conditions + (1 | participant)$. *89% CI not including zero and PP _{$b>0$} below 5.5%
 1115 or above 94.5% (i.e. significant effect).

	Benefit of lip movements		
	<i>b</i>	89% CI	PP _{b>0}
Performance	-0.05	[-0.28, 0.17]	36.09%
Difficulty	0.04	[-0.19, 0.28]	60.86%
Motivation	0.06	[-0.08, 0.19]	76.64%

1116 **Supplementary Table 2.** *Effects of the benefit of lip movements on behavior when the lips are*
1117 *not occluded.*